TAMPEREEN TEKNILLINEN YLIOPISTO
TAMPERE UNIVERSITY OF TECHNOLOGY

OLLI LAHTI

TUBULAR TRUSS GEOMETRY OPTIMIZATION

Master of Science thesis

Examiner: D.Sc. Kristo Mela
Examiner and topic approved by the
Faculty Council of the Faculty of
Business and Built Environment
on 30th October 2017

ABSTRACT

OLLI LAHTI: Tubular Truss Geometry Optimization
Tampere University of Technology
Master of Science thesis, 59 pages, 6 Appendix pages
21.11. 2017
Master's Degree Programme in Civil Engineering
Major: Structural Design
Examiner: D.Sc. Kristo Mela
Keywords: shape optimization, geometry optimization, implicit programming, bilevel programming, roof truss, integer programming

In this study, geometry optimization of tubular roof trusses is investigated. Applicable Eurocode 3 design conditions are presented, which provide the constraints for the problem. Optimized roof truss types are typical, statically determinate lattice structures. Member cross-sections are selected from a discrete set of commercially available profiles.

Mixed integer nonlinear programming problem is obtained. Implicit programming approach is utilized to treat the problem, which is divided into two levels. Sizing problem represents the first level problem which is formulated into the mixed-integer linear programming task. Problem is solved utilizing branch-and-cut algorithm. Geometry optimization represents second level problem which is solved utilizing heuristic algorithm. Output of the optimization process is nodal coordinates and member profiles.

Purpose of the work is to facilitate the implementation of geometry optimization in a design tool. The aim of the optimization is to find a light design. Other goal is to study various procedures to decrease calculation time. Procedures are presented on numerical calculations. A closer look is given at a case study to highlight the crucial factors on geometry optimization.

TIIVISTELMÄ

OLLI LAHTI: Putkiristikon geometrian optimointi
Tampereen teknillinen yliopisto
Diplomityö, 59 sivua, 6 liitesivua
Marraskuu 2017
Rakennustekniikan koulutusohjelma
Pääaine: Rakennesuunnittelu
Tarkastajat: TkT Kristo Mela
Avainsanat:Keywords: geometrian optimointi, implisiittinen ohjelmointi, kattoristikko

Tässä työssä tarkastellaan putkiprofiilista valmistetun kattoristikon geometrian optimointia. Työn tarkoitus on tutkia geometrian optimoinnin soveltuvuutta kattoristikoiden suunnitteluohjelmaan.

Työn ensimmäisessä osassa esitellään kattoristikon yleisiä suunnitteluperiaatteita, jotka toimivat optimoinnin reunaehtoina. Optimoinnin kohteena käytetään yleistä kattoristikkotyyppiä. Ristikko on symmetrinen, yksiaukkoinen ja staattisesti määrätty. Optimoinnin lähtökohtana käytetään konventionaalista geometriaa, jossa yläpaarre on jaettu tasavälisiin osiin.

Optimoinnin tavoitteena on painon minimointi ja rajoitusehtoina käytetään eurokoodin teräsrakenteiden suunnittelukriteereitä, jotka tässä työssä esitellään soveltuvin osin. Optimoinnin tuloksena saadaan solmukoordinaatit ja sauvojen poikkileikkaukset. Poikkileikkaukset valikoituvat diskreetistä profiilikirjastosta. Työn ulkopuolelle rajataan liitosdetaljien tarkastelu.

Optimointitehtävän formuloinnissa hyödynnetään implisiittistä ohjelmointia, jossa tehtävä jaetaan lineaariseen ja epälineaariseen sekaluku tehtävään. Ensimmäinen tehtävä vastaa mitoitusoptimointia ja jälkimmäinen geometrian optimointia. Mitoitusoptimoinnissa hyödynnetään branch-and-cut-algoritmia kun taas geometrian optimointi suoritetaan heuristisella algoritmilla.

Työn eräs tavoite etsiä menetelmiä, jotta intensiivinen laskenta saadaan suoritettua kohtuullisessa ajassa. Kehitetyt 3 heuristista menetelmää esitellään yksityiskohtaisesti. Implementointia tarkastellaan numeeristen laskujen valossa. Työssä tutkitaan kohdefunktion käyttäytymistä ja tarkastellaan laskenta-aikoja. Heuristisia menetelmiä verrataan tulosten valossa keskenään. Lisäksi poimitaan yksi laskentatapaus tarkempaan tarkasteluun. Painon muutokseen vaikuttavat tekijät tuodaan esille ja vedetään johtopäätöksiä laskentatapausten minimointia ohjaavista tekijöistä.

PREFACE

This study was conducted from the end of January to mid November in 2017. During the year 2016 I was looking for a topic for my master's thesis. I was introduced to the structural optimization by Adjunct Professor Kristo Mela (Department of Civil Engineering, TUT) which gave rise to my fascination for the subject. At the beginning of the 2017, new research project was instigated by SSAB and Adjunct Professor Mela and I was given a chance to take part in the project. The idea for geometry optimization of roof trusses came from my supervisor, Adjunct Professor Mela. Implicit programming approach utilizing mixed integer programming was chosen as the first technique to be studied. As spring went on, it became clear that chosen approach was to be the main direction of the study.

The funding was provided by SSAB and I would like to thank Jussi Minkkinen and Petteri Steen immensely for giving me the opportunity to conduct this study.

I'm forever grateful to Adjunct Professor Mela for guiding me into the realm of structural optimization in his professional supervision. It has been truly a privilege.

I would also like to thank fellow students Miro Kierros and Mika Helminen and researcher Teemu Tiainen for their help and peer support.

To my father in a far-off Rovaniemi. Thank you for never giving up the hope.

Lastly and most importantly, I would like to express my deepest gratitude to my beloved ones, Seela and Nina.

Tampere, 21.11.2017

Olli Lahti

CONTENTS

LIST OF ABBREVIATIONS AND SYMBOLS

Abbreviations

MILP	Mixed-integer linear problem
MINLP	Mixed-integer nonlinear problem
NAND	Nested analysis and design
RHS	Rectangular hollow section
SHS	Square hollow section

Cross-section

A	area of the profile [mm^2]
b	width [mm]
E	elastic modulus
f_y	yield strength [kN/mm^2]
h	height [mm]
I	moment of inertia of the profile [mm^4]
M_{Ed}	design value of bending moment [kN/mm]
$M_{p,Ed}$	design value of bending moment acting on a point [kN/mm]
r	corner rounding [mm]
t	wall thickness [mm]
W_{pl}	is plastic section modulus [mm^3]
ρ	density of the profile [kg/mm^3]
α	imperfection factor in buckling

Sets

$\mathcal{D}$	displacement degrees of freedom
$\mathcal{D}_{GV}$	geometry variation degrees of freedom
$\mathcal{M}$	truss members
$\mathcal{M}_{UC}$	upper chord members
$\mathcal{M}_{LC}$	lower chord members
$\mathcal{M}_{BR}$	brace members
$\mathcal{M}_{\ell}$	members connnected to node ℓ
$\mathcal{M}_{adj}$	adjacent members
$\mathcal{N}$	nodes

$\mathcal{N}_{UC}$	upper chord nodes
$\mathcal{N}_{LC}$	lower chord nodes
$\mathcal{P}$	profiles
$\mathcal{P}_{UC}$	upper chord profiles
$\mathcal{P}_{LC}$	lower chord profiles
$\mathcal{P}_{BR}$	brace profiles
$\mathcal{P}_{BR,B}$	brace profiles in procedure B
$\mathcal{P}_{BR,C}$	brace profiles in procedure C
$\mathcal{P}_{BR,D}$	brace profiles in procedure D
$\mathcal{P}_{BR,T}$	brace profiles of turss T
Ω_{Sizing}	feasible set for sizing optimization
Ω_{Geom}	feasible set for sizing optimization

Variables

$\Delta\mathbf{X}$	geometry variable vector
y_{ij}	profile selection variable
$\mathbf{y}$	profile selection variable vector
N_{ij}	normal force variable
$\mathbf{N}$	normal force variable vector
u_ℓ	displacement of node ℓ
$\mathbf{u}$	displacement variable vector

Coordinates

$\mathbf{X}$	nodal coordinates
$\mathbf{X}^0$	nodal coordinates of initial geometry
$\mathbf{X}^*$	nodal coordinates of optimum geometry
$\mathbf{X}^r$	nodal coordinates in iteration r
$\mathbf{v}_d$	direction vector of geometry variable d

Loads

$\mathbf{p}$	load vector of nodal forces
$\mathbf{m}$	load vector of nodal moments
$\mathbf{q}$	load vector of equivalent nodal forces from line loading

Numbers

n_d	Number of degrees of freedom in sizing problem
n_M	Numbers of elements (members)
n_L	Number loading conditions
n_x	Number sizing variables
n_{Pi}	Number of profiles of member i
$n_{p,\ell}$	Number of the profiles of the profile group ℓ
n	Number of nodes
n_{GV}	Number of the geometry variation variables
$n_{N,d}$	number of geometry variation nodes corresponding to the $d \in \mathcal{D}_{GV}$
n_{div}	Number of half span upper chord division

Roof truss

h_1	which is truss height at the support
h_2	truss height at the ridge
$slope$	roof slope
θ_{incl}	roof inclination angle
$\theta_{\ell,mn}$	angle between members m and n connected by node ℓ
L	truss span

Mechanics

$\mathbf{B}_g$	self weight matrix
$\mathbf{B}$	statics matrix

1. INTRODUCTION

1.1 General Problem Description

The premise for the design of typical roof truss structures is presented in the Figure 1.1. Supporting structure is needed to bear the vertical loading. Rough geometric properties, such as span and roof slope, as well as loading conditions are provided as a basis for the design. In this thesis, similar premise is adopted.

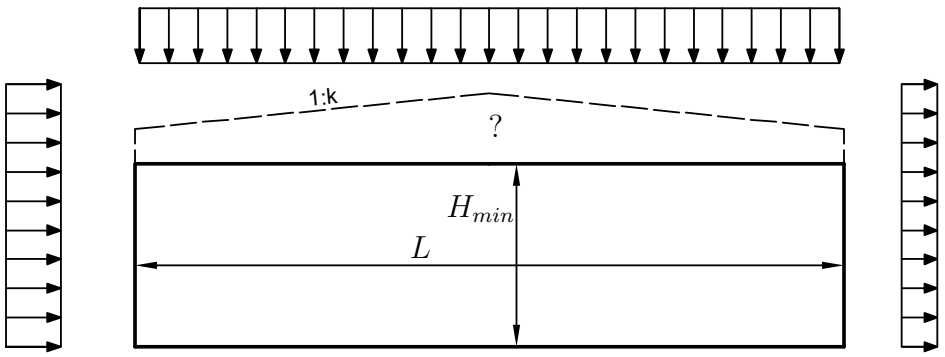

Figure 1.1 *Basis of the truss design.*

Typically height of the truss is chosen between $L/16 \cdots L/9$ depending on loading conditions, span, local design conventions etc. Also, only external loads, shown in Figure 1.1, are known *a priori*. Here, by external loads, snow load, self weight of a secondary roof structure etc. are ment. In other words, truss self weight is not known before the design process. This approach is adopted in this study. Typical lattice structures are simply supported, symmetrical K, KT and N type trusses, which are illustrated in Figure 1.2.

Figure 1.3 shows welded Y-, K-, KT and T-type joints which are typical joint types in above-mentioned tubular lattice structures.

In tubular structures, cross-section profiles are normally selected from manufacturer

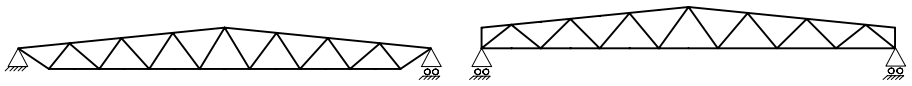

(a) K truss

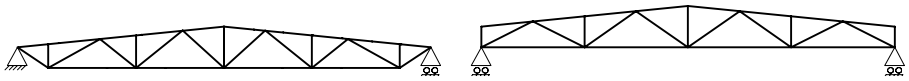

(b) KT truss

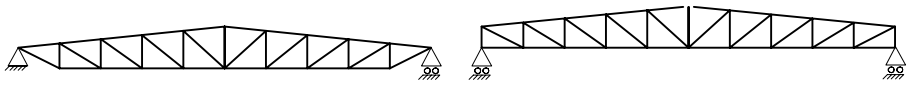

(c) N truss

Figure 1.2 *Truss types*

(a) Y-joint **(b)** K-joint

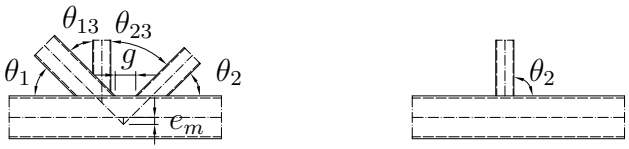

(c) KT-joint **(d)** T-joint

Figure 1.3 *Joint types*

catalogs. It is also common, that profile type is square hollow section (SHS). Most common steel grades are mild steels, such as S355 or S420. Usage of high strength steels (HSS), such as S460, S500 S550 and S700, is also possible.

Conventional design process, generally, proceeds as follows: Initial design is first selected based on above described design premises, designers knowledge, design guides, prevailing conventions, demands of customer, manufacturing and erection process etc. Then, structural strength, displacement and other applicable conditions are checked in all loading cases. Necessary corrections are made on the structure and conditions are checked again. Thus, the process is iterative by its nature. In this thesis, the design process is simulated and automated.

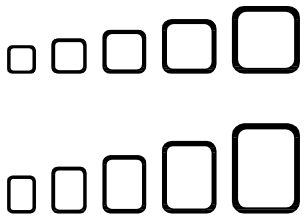

Figure 1.4 *Cross-section profiles.*

The general goal of the truss design process is to produce necessary information for manufacturing and erecting an economical truss. The information includes

- Truss geometry
- Bar profiles
- Joint details

as presented in Figure 1.5. Here, truss geometry means member positions. Also other information is needed, such as details about painting, fire protection etc.

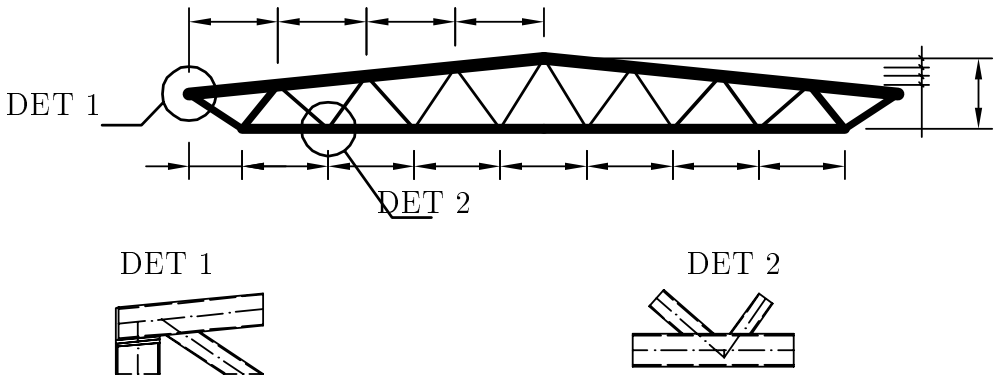

Figure 1.5 *Truss design information.*

1.2 Literature review

1.2.1 Truss optimization

One of the earliest efforts in truss optimization in which not only sizes of the members but also nodal coordinates were determined, while considering stress constraints, was presented by Dorn et al. (1964). Also, Pedersen (1972) addressed truss weight optimization where bar areas and joint locations were allowed to change. Analytical expressions of Pedersen (1972) included partial derivatives determined for the problem solving. Also, cross-section and nodal coordinate variables were continuous. Multiple load cases were also included in the problem. Early problem formulations were typically based on approach, where equations of equilibrium were brought into the problem as equality constraints. This is called *simultaneous analysis and design* (SAND) approach. Presentation can be found in text book of Hafka and Gürdal (1992). Equations of equilibrium typically were nonlinear which led to non linear programming (NLP) problem. Problem then were solved using deterministic algorithms.

Practical design problems generally involve discrete design parameters. Problem evolves into a mixed-integer nonlinear programming (MINLP) problem. Early consideration of this problem type and suitable formulation for a truss structure including discrete cross-section variables has been presented by Grossmann et al. (1992). Formulation was developed further by Rasmussen and Stolpe (2008), who introduced linear inequalities and disaggregated the material law from the equilibrium equations. The problem formulation was for topology optimization. Buckling constraints were brought to the MILP truss topology optimization problem by Mela (2014).

Branch-and-cut method is efficient in solving mixed integer linear problems. Wolsey (1998) provides a text book presentation of integer programming and cutting plane methods for linear problems that is succesfully implemented by Rasmussen and Stolpe (2008).

1.2.2 Implicit programming approach

The principle of implicit programming approach is simple (see e.g.(Achtziger 2007). Consider a problem of two types of variables $\mathbf{x}$ and $\mathbf{y}$. If for fixed $\mathbf{x}$ the problem has a unique solution $\mathbf{y}$, then $\mathbf{y}$ can be interpreted as a function of $\mathbf{x}$ and whole problem can be formulated with respect to the "master variable" $\mathbf{x}$. Kirsch (1981) considered

a geometry optimization problem with continuous cross-section and node coordinate variables. Problem is divided in two different design spaces, where nodal coordinates become independent variables, i.e. *master variables*, and design variables are solved for fixed geometry. Achtziger (2007) proposes a formulation for simultaneous optimization of truss geometry and topology utilizing compliance minimization that combines continuous volume constraints with continuous cross-section variables.

1.3 Scope and Aims of the Thesis

Investigation into the generation of light tubular roof truss structures is the main focus of this thesis. Furthermore, it is imperative, that obtained designs comply with prevailing building codes. Hence, the objective is to find

- minimum weight roof truss design

which fulfils

- Eurocode 3 member strength conditions
- Eurocode 3 member stability conditions
- applicable joint design conditions

Member profiles are selected from

- commercially available discrete selection.

High-strenth steel (HSS) profiles are also included in the study to investigate the HSS usage in roof trusses. Method for determining the minimum weight design is chosen to be

- geometry optimization.

In this thesis, a mixed integer linear programming (MILP) formulation, proposed by Mela (2013) for truss topology optimization, is utilized and modified for sizing optimization. Implicit programming approach is employed in geometry optimization.

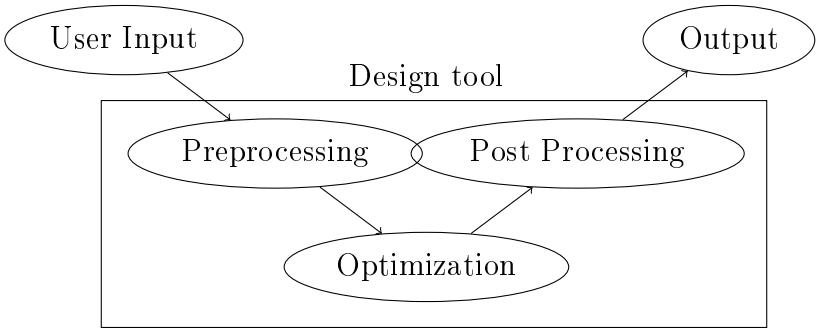

Figure 1.6 *Design procedure.*

The studied implementation is designed to be a part of the design process. However, due to chosen method, all applicable design conditions cannot be included in the optimization problem. Therefore the design procedure is assumed to be divided in preprocessing, optimization and postprocessing phase (see Figure 1.6). In preprocessing, initial information is collected for the optimization phase. In optimization the problem is solved and resulting design is sent to postprocessing phase, where final checking and necessary corrections are made. The scope of this thesis is optimization phase. Output of the optimization is optimum design, which refers to nodal coordinates and member profiles. Thus, optimization does not provide joint details.

Furthermore, the goal is to examine alternative optimization procedures to keep the calculation time "acceptable". Thus, time limit is imposed to the problem solving.

2. DESIGN OF TUBULAR ROOF TRUSS STRUCTURES

2.1 Initial Geometry

Initial geometries are generated according to the following principles. Vector of initial nodal coordinates, i.e. *initial geometry*, is denoted by $\mathbf{X}^0$. It is assumed that upper chord half span is divided in segments of equal length. This is called *division*. Also, truss is assumed to be symmetric with respect to the midspan. This is shown in Figure 2.1.

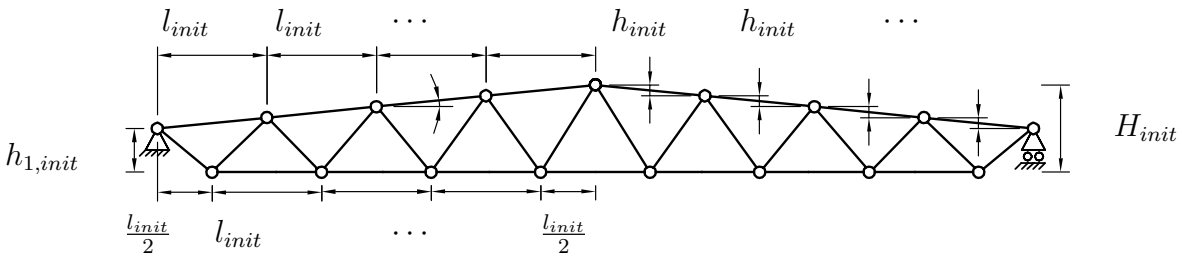

Figure 2.1 *Truss geometry initialization.*

Horizontal distance between upper chord nodes is derived

$$l_{init} = \frac{0.5 \cdot L_{init}}{n_{div}}, \tag{2.1}$$

where L_{init} is the span of the initial truss and n_{div} refers to the upper chord division for the half span. Truss height at the support is calculated by

$$h_{1,init} = H_{init} - \tan\theta_{UC} \frac{L_{init}}{2}, \tag{2.2}$$

where H_{init} is the height of the truss with initial geometry, and where $\tan\theta_{UC}$ is the slope of the roof as θ_{UC} refers to the upper chord inclination angle. Height increment is calculated by

$$h_{init} = \tan\theta_{UC} \frac{0.5 L_{init}}{n_{div}}. \tag{2.3}$$

2.2 Structural Analysis

Eurocode provides guidance and regulations for the structural analysis of truss structures (EN 1993–1–8 2005). The distribution of axial forces in a lattice girder may be determined on the assumption that the members are connected by pinned joints. Secondary moment at the joint may be neglected both in the design of tension chord members and brace members as well as in the design of the joints, provided that conditions for joint eccentricity

$$-0.55h_0 \leq e \leq 0.25h_0 \tag{2.4}$$

are satisfied. Above, h_0 refers to the height of the chord member. Nevertheless, the moments resulting from the eccentricities should be taken into account in the design of compression chord members.

The moments resulting from transverse loads (whether in-plane or out-of-plane) that are applied between panel points, should be taken into account in the design of the members to which they are applied. The brace members may be considered as pin-connected to the chords, so moments resulting from transverse loads applied to chord members need not be distributed into brace members, and vice versa. The chords may be considered as continuous beams, with simple supports at panel points.

However, different approach is assumed in this study. In static model, all the members are modelled as pin-jointed bar elements. This is shown in Figure 2.2. Only axial forces are obtained from this model. Therefore, to take into account the bending moments resulting from the transverse loading, approximative estimations must be applied. These are covered later in the Section 2.7. Since the joint eccentricities are not known "a priori", moments resulting from the joint eccentricities are neglected in the optimization implementation.

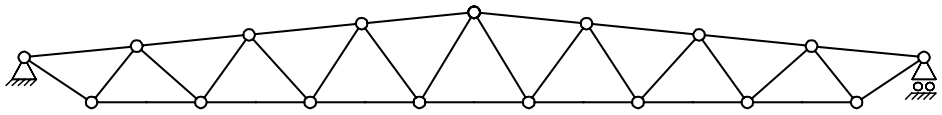

Figure 2.2 *Pin-jointed analysis model.*

Also following condition concerning the length of the members with respect to the side length shall be satisfied

$$\frac{L_i}{h_i} \geq 6 \tag{2.5}$$

This is stated in EN 1993–1–8 (2005) Clause 5.1.5(3).

2.3 Cross-sections

Cross-section profiles are selected from standard industrial catalog. Unique profile selection is allocated for each member group. As joint types are determined before optimization, group profile selection is limited to one satisfying Eurocode joint requirements presented in section 2.4.

Plastic cross-section resistances are utilized in this work. Therefore, compressed parts of the cross-sections must fulfil the condition

$$\frac{c_i}{t_i} \leq 38\sqrt{\frac{235}{f_y}} \tag{2.6}$$

This is stated in EN 1993–1–1 (2005) Table 5.2

2.4 Design of Joints

Each joint type is determined according to the selected topology of the initial structure. The welds are assumed to have equal strength with the member and weld type is assumed to be fillet weld. Thus, the strength of the welds are not considered in this work. Joint resistances are not known *a priori*. Moreover, expressions for the joint resistances are partially nonlinear with respect to problem variables presented in Chapter 3. Therefore in this work, joint strength requirements are not fully, but partially implemented in the optimization phase. However, general design rules of the joints are implemented in the optimization as presented in this section.

Due to welding requirements, angles $\theta_{\ell,mn}$ between adjacent members i_m and i_n connected by the joint ℓ, must fulfil the condition

$$\theta_{\ell,mn} \geq 30^\circ \tag{2.7}$$

Moment from the joint eccentricity is not implemented in this work.

2.5 Joint Resistance

2.5.1 General

The design values of the internal axial forces and design resistances of the joints both in the brace members and in the chords at the ultimate limit state should fulfil

the condition

$$-N_{\mathrm{Rd}} \leq N_{\mathrm{Ed}} \leq N_{\mathrm{Rd}} \tag{2.8}$$

where N_{Rd} refers to the axial force resistances of the joints and N_{Ed} to the design values the axial forces of the members. Failure modes are presented in Figure 2.3. As stated earlier, all the joint strength conditions are not considered. Therefore in this section, only applicable strength requirements are shown.

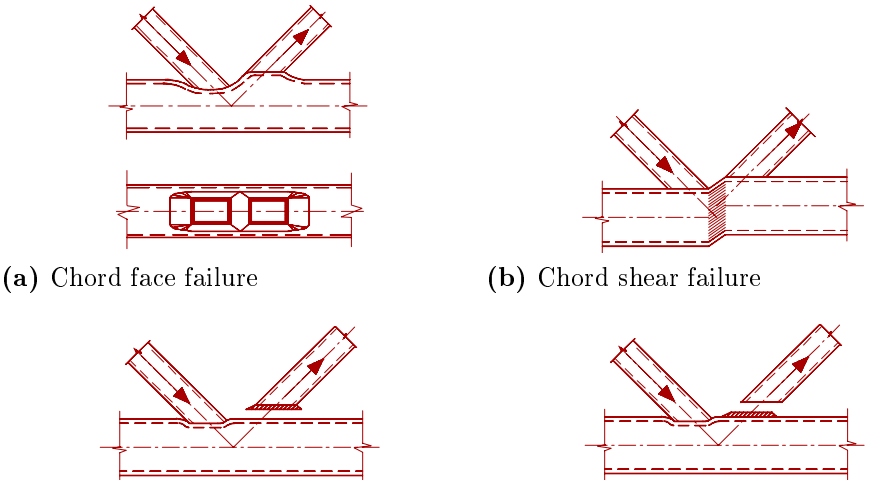

(a) Chord face failure **(b)** Chord shear failure

(c) Punching shear **(d)** Brace failure

Figure 2.3 *Failure modes for hollow section joints (EN 1993-1-8 2005).*

2.5.2 T-, and Y-joints

For T- and Y-joints no failure modes are considered.

To simplify code checking following validity checks must be made

$$0.25 \leq \frac{b_i}{b_0} \leq 0.85 \tag{2.9}$$

$$\frac{b_i}{t_i} \leq 35 \tag{2.10}$$

$$\frac{h_i}{t_i} \leq 35 \tag{2.11}$$

$$0.5 \leq \frac{h_0}{b_0} \leq 2.0 \tag{2.12}$$

$$0.5 \leq \frac{h_i}{b_i} \leq 2.0 \tag{2.13}$$

$$\frac{b_0}{t_0} \leq 35 \tag{2.14}$$

$$\frac{h_0}{t_0} \leq 35 \tag{2.15}$$

where b_0 and b_i denote chord and brace profile widths, respectively. Also, h_0 and h_i refer to respective chord and brace profile heights. Furthermore, t_0 and t_i denote respective chord and brace member wall thicknesses.

2.5.3 K- and N-joints

Validity conditions for all members belonging to a K- and N-joint are

$$\max\left\{0.35\,,\,0.1+0.01\frac{b_0}{h_0}\right\} \leq \frac{b_i}{b_0} \leq 0.85 \tag{2.16}$$

$$\frac{b_i}{t_i} \leq 35 \tag{2.17}$$

$$\frac{h_i}{t_i} \leq 35 \tag{2.18}$$

$$0.5 \leq \frac{h_0}{b_0} \leq 2.0 \tag{2.19}$$

$$0.5 \leq \frac{h_i}{b_i} \leq 2.0 \tag{2.20}$$

$$\frac{b_0}{t_0} \leq 35 \tag{2.21}$$

$$\frac{h_0}{t_0} \leq 35 \tag{2.22}$$

Since the cross-sections are belonging to the cross-section class 1 or 2, as was required in Section 2.3, only Eqs. (2.9) and (2.16) are implemented. Other joint side length conditions presented in Eqs. (2.10)–(2.22), are automatically fulfilled when cross-

section class requirements are met.

Chord shear

Resistance of the chords (see EN 1993–1–8 (2005)) for this failure mode is calculated by

$$N_{\mathrm{j,0,Rd}} = \left((A_0 - A_v) f_{\mathrm{y},0} + A_v f_{\mathrm{y},0} \sqrt{1 - \frac{V_{\mathrm{Ed}}}{V_{\mathrm{pl,Rd}}}^2} \right) \cdot \frac{1}{\gamma_{\mathrm{M5}}} \tag{2.23}$$

According to the EN 1993–1–12 (2005), for steel grades with yield strength above 355 MPa, resistances should be reduced by a factor 0.9 and for steel grades with yield strength above 460 MPa up to the 700 MPa, resistances should be reduced by the a factor 0.8. Near the mid-span, brace members have very small normal forces and consequently shear forces in joints close to mid-span are also very small. Thus, value $V_{\mathrm{Ed}} \approx 0$ and above mentioned reduction factors are plugged into the Eq. (2.23), which yields

$$N_{\mathrm{j,0,Rd}} = \begin{cases} 0.9 \dfrac{A_0 f_{\mathrm{y},0}}{\gamma_{\mathrm{M5}}}, \text{ when } 355\mathrm{MPa} < f_{\mathrm{y},0} \leq 460\mathrm{MPa} \\ 0.8 \dfrac{A_0 f_{\mathrm{y},0}}{\gamma_{\mathrm{M5}}}, \text{ when } 460\mathrm{MPa} < f_{\mathrm{y},0} \leq 700\mathrm{MPa} \end{cases} \tag{2.24}$$

It can be seen, that the equations above present in fact the chord axial strength multiplied by reduction factors and therefore must be included in the chord axial strength conditions.

2.6 Member Resistance

The resistance of the members subjected to axial force (EN 1993–1–1 2005) is checked as follows

$$\frac{N_{\mathrm{Ed}}}{N_{\mathrm{Rd}}} \leq 1 \tag{2.25}$$

where cross-section resistance can be calculated by

$$N_{\mathrm{Rd}} = \frac{A f_{\mathrm{y}}}{\gamma_{\mathrm{M0}}} \tag{2.26}$$

Furthermore, resistance for combined bending and axial force must fulfil the condition

$$\frac{M_{\mathrm{Ed}}\gamma_{\mathrm{M0}}}{W_{\mathrm{pl}}f_{\mathrm{y}}\left(1-n\right)\left(1-0.5a_w\right)} \leq 1 \tag{2.27}$$

where

$$a_w = \min\{\frac{(A-2bt)}{A}, 0.5\} \tag{2.28}$$

and

$$n = \frac{N_{\mathrm{Ed}}}{Af_{\mathrm{y}}} \tag{2.29}$$

By plugging Eqs. (2.28) and (2.29) into the Eq. (2.27) and reformulating it yields

$$N_{\mathrm{Ed}} \leq \chi_{MN} A f_{\mathrm{y}} \tag{2.30}$$

where

$$\chi_{MN} = 1 - \frac{r_M}{1-0.5a_w} \tag{2.31}$$

Utility ratio of bending moment can be expressed as

$$r_M = \frac{M_{\mathrm{y,Ed}}\gamma_{\mathrm{M1}}}{W_{\mathrm{y,pl}}f_{\mathrm{y}}} \tag{2.32}$$

Here, due to the pin jointed structural model, the static analysis only yields axial forces of the members. Therefore, estimation of the actions due to the bending moment of the members subject to the transversal loading, is made. As a rule of thumb, design bending moment is assumed to be

$$M_{\mathrm{y,Ed}} = \frac{1}{10} q_{Ed} l_i^2. \tag{2.33}$$

Also, the effect of the bending moment from the eccentricity at the support is taken into account. Estimation for the action is made as it is not included in the structural model. Estimation for the support moment is

$$M_{\mathrm{p,Ed}} = 1.05e \cdot R_{sup} \tag{2.34}$$

where,

$$R_{sup} = q_{Ed} \cdot \frac{L}{2} \tag{2.35}$$

and where e is approximated eccentricity of the support reaction. The bending moment of Eq. (2.34) is added to the upper chord member connected with the support.

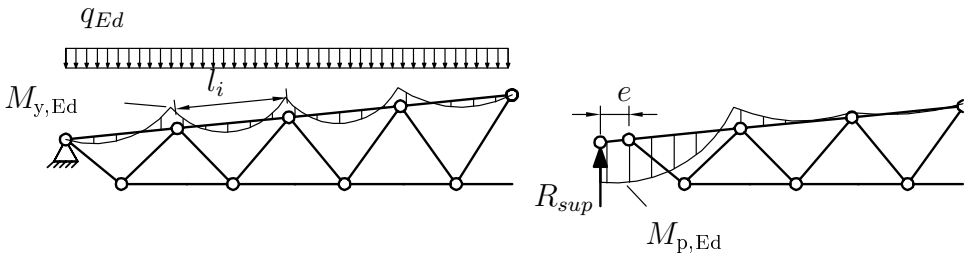

Figure 2.4 *Bending moment.*

2.7 Member Stability

According to EN 1993–1–1 (2005, Sec. 6.3), the flexural buckling resistance reads as:

$$-\frac{N_{\mathrm{Ed}}\gamma_{\mathrm{M1}}}{\chi A f_{\mathrm{y}}} \leq 1 \tag{2.36}$$

$$\chi = \frac{1}{\Phi + \sqrt{\Phi^2 + \bar{\lambda}^2}} \tag{2.37}$$

$$\bar{\Phi} = 0.5(1 + \alpha(\bar{\lambda} - 0.2) + \bar{\lambda}^2) \tag{2.38}$$

$$\bar{\lambda} = \sqrt{\frac{A f_{\mathrm{y}}}{N_{\mathrm{cr}}}} \tag{2.39}$$

$$N_{\mathrm{cr}} = \pi^2 \frac{EI}{L_n^2} \tag{2.40}$$

where value $L_n = 0.9L$ is used for the braces and chords.

For chord members subjected to bending and flexural buckling (compression), following design conditions shall be checked:

$$-\frac{N_{\mathrm{Ed}}\gamma_{\mathrm{M1}}}{\chi_y A f_{\mathrm{y}}} + k_{yy}\frac{M_{\mathrm{y,Ed}}\gamma_{\mathrm{M1}}}{W_{\mathrm{y,pl}} f_{\mathrm{y}}} \leq 1 \tag{2.41}$$

$$-\frac{N_{\mathrm{Ed}}\gamma_{\mathrm{M1}}}{\chi_z A f_{\mathrm{y}}} + k_{zy}\frac{M_{\mathrm{y,Ed}}\gamma_{\mathrm{M1}}}{W_{\mathrm{y,pl}} f_{\mathrm{y}}} \leq 1 \tag{2.42}$$

where

$$k_{yy} = \min \begin{cases} C_{\mathrm{my}}\left(1 + \left(\bar{\lambda}_y - 0.2\right)\frac{N_{\mathrm{Ed}}\gamma_{\mathrm{M1}}}{\chi_y N_{\mathrm{Rk}}}\right) \\ C_{\mathrm{my}}\left(1 + 0.8\frac{N_{\mathrm{Ed}}\gamma_{\mathrm{M1}}}{\chi_y N_{\mathrm{Rk}}}\right) \end{cases} \tag{2.43}$$

and

$$k_{zy} = 0.6\, k_{yy} \tag{2.44}$$

In Eq. (2.42), axial force was given a negative sign to assure, that axial force and bending moment does not cancel each other out. In all calculations estimated bending moment is set positive.

Equivalent uniform moment factor C_{my} is obtained from

$$C_{\mathrm{my}} = \begin{cases} \max\left(0.2 + 0.8\alpha_s, 0.4\right) & \text{when} \quad 0 \leq \alpha_s \leq 1 \\ \max\left(0.1 - 0.8\alpha_s, 0.4\right) & \text{when} \quad -1 \leq \alpha_s \leq 0 \end{cases} \tag{2.45}$$

where

$$\alpha_s = \frac{M_s}{M_h} \tag{2.46}$$

As the moment field of the members subject to the transversal line loading is not known *a priori*, conservative assumptions are made to simplify calculations. By presuming $\alpha_s = 1$, and substituting that into the above equation 2.45 yields maximum value $C_{\mathrm{my}} = 1$. By substituting the equations 2.41, 2.42, 2.43 and 2.44, plugging

$C_{\mathrm{my}} = 1$ into the equations and reformulating them yields

$$N_{\mathrm{Ed}} \leq \chi_{Mb} f_{\mathrm{y}} A \tag{2.47}$$

where

$$\chi_{Mb} = \min \begin{cases} \chi_y \left(\dfrac{1 - r_M}{1 + b_M r_M} \right) \\ \chi_z \left(\dfrac{1 - 0.6 r_M}{1 + 0.6 b_M r_M} \right) \end{cases} \tag{2.48}$$

and where

$$r_M = \frac{M_{\mathrm{y,Ed}} \gamma_{\mathrm{M1}}}{W_{\mathrm{y,pl}} f_{\mathrm{y}}} \tag{2.49}$$

$$b_M = \min \begin{cases} \bar{\lambda}_y - 0.2 \\ 0.8 \end{cases} . \tag{2.50}$$

3. PROBLEM FORMULATION

In this chapter formulation for roof truss geometry optimization problem is presented. First MINLP problem is introduced. Then treatment of the problem through implicit programming approach is demonstrated, which includes presenting geometry optimization formulation and sizing optimization formulation.

Joint strength constraints are nonlinear, and they are therefore not incorporated into the mixed-integer linear programming problem. For the same reason secondary moment from the joint eccentricity is also not considered. Furthermore, shear strength constraints are left out of the problem. Also, chord chord bending moment is approximated.

3.1 Introduction

In direct form, geometry optimization problem reads as

$$\begin{aligned} \underset{\mathbf{x},\Delta\mathbf{X}}{\text{minimize}} \quad & \mathbf{c}^T\mathbf{x} \\ \text{such that} \quad & \mathbf{A}(\Delta\mathbf{X})\,\mathbf{x} \leq \mathbf{b} \\ & \mathbf{Aeq}(\Delta\mathbf{X})\,\mathbf{x} = \mathbf{beq} \\ & \underline{\mathbf{x}} \leq \mathbf{x} \leq \overline{\mathbf{x}} \\ & \mathbf{g}(\Delta\mathbf{X}) \leq \mathbf{0} \\ & \underline{\Delta\mathbf{X}} \leq \Delta\mathbf{X} \leq \overline{\Delta\mathbf{X}} \end{aligned}, \tag{3.1}$$

where $\Delta\mathbf{X} = \{X_1, X_2, \dots\}$ represent nodal coordinate variation and is therefore referred as *geometry variation variables* i.e. *nodal coordinate variation variables*. These variables are continuous. Denotation $\mathbf{x} = \left\{\mathbf{y}, \mathbf{N}^1, \mathbf{N}^2, \cdots, \mathbf{N}^k, \mathbf{u}^k\right\}$ is representing *sizing variables*, where $\mathbf{y}$ are binary cross-section selection variables, $\mathbf{N}^1, \mathbf{N}^2, \cdots, \mathbf{N}^{n_L}$ are continuous member force variables corresponding to the load cases $k = 1, 2, \cdots, n_L$ and where $\mathbf{u}^k$ are n_L vectors of continuous nodal displacement variables. Each vector is corresponding to a loading case. Cross-section selection variables can also be referred as design variables and member force and nodal displacement variables as state variables.

Furthermore, $\mathbf{A}$ and $\mathbf{Aeq}$ are representing inequality and equality constraints as well as $\underline{\mathbf{x}}, \overline{\mathbf{x}}$ lower and upper bounds for the sizing variables. Above constraints are considered as *sizing constraints* and define a feasible set denoted by Ω_{Sizing}. Moreover, $\mathbf{g}$ is presenting inequality constraints and $\underline{\Delta\mathbf{X}}, \overline{\Delta\mathbf{X}}$ lower and upper bounds for the nodal coordinate variation variables. Later constraints are considered as *geometry constraints* and define a feasible set denoted by Ω_{Geom}. Vector $\mathbf{g}$ is a function of $\Delta\mathbf{X}$ only and can also be nonlinear.

Notice, that the majority of the constraints are a function of geometry variation variables, as those constraints are dependent of the member lengths and angles, which on the other hand are dependent on the nodal coordinates of the truss. Also, most of the constraints are nonlinear with respect to the $\Delta\mathbf{X}$. Thus, above problem can be classified as mixed integer nonlinear problem (MINLP).

It turns out, that the direct treatment of the problem in hand is complex (Achtziger 2007). Consequently, different approach is adopted. The problem is treated in two phases. For fixed geometry $\Delta\mathbf{X} = \Delta\hat{\mathbf{X}}$, problem reduces to

$$\begin{aligned} \underset{\mathbf{x}}{\text{minimize}} \quad & \mathbf{c}^T\mathbf{x} \\ \text{such that} \quad & \mathbf{A}(\Delta\hat{\mathbf{X}})\,\mathbf{x} \leq \mathbf{b} \\ & \mathbf{Aeq}(\Delta\hat{\mathbf{X}})\,\mathbf{x} = \mathbf{beq} \\ & \underline{\mathbf{x}} \leq \mathbf{x} \leq \overline{\mathbf{x}} \end{aligned} \tag{3.2}$$

which represents sizing optimization problem. Also, all remaining (sizing) constraints become linear. Thus, the problem reduces to mixed-integer linear programming problem (MILP), which has, when solvable, a unique solution (Wolsey 1998). Then it can be solved to the global minimum effectively. Problem 3.2 for fixed geometry is denoted by $\Phi(\Delta\mathbf{X}_0)$. If for the fixed geometry ($\mathbf{X} = \hat{\mathbf{X}}$), the remaining sizing problem 3.2 possesses a unique solution, then $\mathbf{x}$ can be interpreted as a function of $\Delta\mathbf{X}$ and problem 3.1 can be formulated as a problem of "master variable" $\Delta\mathbf{X}$ only, also referred as upper level problem, and the sizing step, which is also referred as the lower level problem (Achtziger 2007). Hence, the problem 3.1 can be reformulated as

$$\begin{aligned} \underset{\Delta\mathbf{X}}{\text{minimize}} \quad & \Phi(\Delta\mathbf{X}) \\ \text{such that} \quad & \mathbf{g}(\Delta\mathbf{X}) \leq \mathbf{0} \\ & \underline{\Delta\mathbf{X}} \leq \Delta\mathbf{X} \leq \overline{\Delta\mathbf{X}} \end{aligned} \tag{3.3}$$

where

$$\Phi(\Delta\mathbf{X}) = \left\{ \begin{array}{ll} \inf\limits_{\mathbf{x}} & \mathbf{c}^T\mathbf{x} \\ \text{such that} & \mathbf{A}(\Delta\mathbf{X})\,\mathbf{x} \leq \mathbf{b} \\ & \mathbf{Aeq}(\Delta\mathbf{X})\,\mathbf{x} = \mathbf{beq} \\ & \underline{\mathbf{x}} \leq \mathbf{x} \leq \overline{\mathbf{x}} \end{array} \right\} \tag{3.4}$$

Equation 3.3 represents geometry variation and can be interpreted as upper level problem. The latter equation 3.4 represents fixed geometry sizing optimization problem and can be interpreted as sizing problem where operator "inf" stands for the greatest lower bound.

By convention we set $\Phi(\Delta\mathbf{X}) = \infty$, if and only if the problem 3.2 does not have feasible solution (see e.g. Achtziger 2007). In numerical calculations, ∞ is replaced by "big number". By doing this it is assured that the geometry variation problem is defined in all of it's domain Ω_{Geom} and operator "inf" can be interpreted as "minimization".

Hence, solving of the problem reduces to the minimization of the geometry variation problem with respect to the $\Delta\mathbf{X}$ where during the minimization the objective function must be repeatedly evaluated, and the evaluation of the geometry variation objective function for the iteration point $\Delta\mathbf{X} = \Delta\mathbf{X}^r$ involves in fact the solving of the sizing problem for the fixed geometry $\Delta\mathbf{X} = \Delta\mathbf{X}^r$. The procedure is also illustrated in the Figure 3.1.

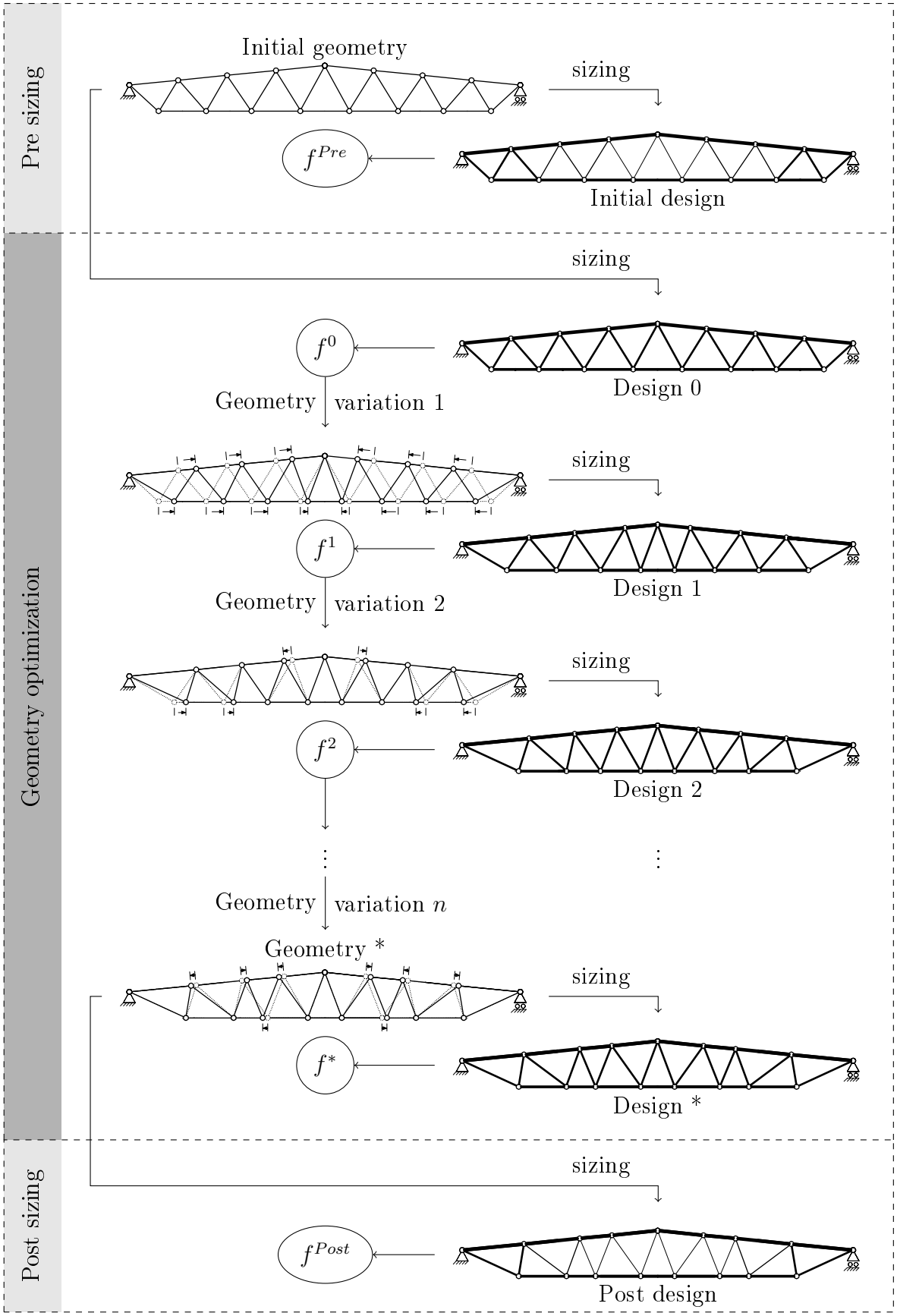

Figure 3.1 *Optimization procedure.*

3.2 Sizing optimization

General formulation for sizing problem is stated as

$$\min_{\mathbf{x}\in\Omega_{Sizing}} f(\mathbf{x}) \tag{3.5}$$

where Ω_{Sizing} is the feasible set (constraints) as represented in Section 3.2.2 and Section 3.2.6, $f(\mathbf{x})$ is objective function as presented in section 3.2.7 and $\mathbf{x}$ is variable vector consisting of design variables and state variables as presented below in section 3.2.1. Solution to the sizing problem yields optimum profiles for fixed geometry. Therefore, in literature this optimization type is often referred as "sizing optimization" (see e.g. Mela 2013).

In sizing problem, nodal equality equations (structural analysis) are included in problem formulation. Thus, separate structural analysis before optimization is not needed as the state variables (normal forces and nodal displacements) are included in the problem formulation and solved as part of the problem solution. In the literature this formulation is therefore often referred as simultaneous analysis and design (SAND) -formulation (Ghattas and Grossmann 1991). More particularly, in this implementation the state variables are continuous and design variables (profile selection variables) discrete. Treatment is therefore called "MILP" -formulation (mixed integer linear programming), which is an instance of a SAND -formulation.

As a result of sizing problem formulation, i.e. mixed integer linear problem formulation, the standard form is obtained. It states as

$$\begin{aligned} \underset{\mathbf{x}}{\text{minimize}} \quad & \mathbf{c}^T\mathbf{x} \\ \text{such that} \quad & \mathbf{A}\,\mathbf{x} \leq \mathbf{b} \\ & \mathbf{Aeq}\,\mathbf{x} = \mathbf{beq} \\ & \underline{\mathbf{x}} \leq \mathbf{x} \leq \overline{\mathbf{x}} \end{aligned} \quad . \tag{3.6}$$

3.2.1 Variables

Variables of a sizing optimization problem and respective numbers are presented in Table 3.1.

Vector of design variables is of following form

$$\mathbf{x} = \left\{\mathbf{y}\,\mathbf{N}_1^1\,\mathbf{N}_2^1 \cdots \mathbf{N}_{n_M}^1\,\mathbf{u}^1 \cdots \mathbf{N}_1^{n_L}\,\mathbf{N}_2^{n_L} \cdots \mathbf{N}_{n_M}^{n_L}\,\mathbf{u}^1\,\mathbf{u}^2, \cdots \mathbf{u}^{n_L}\right\} \tag{3.7}$$

Table 3.1 *Sizing optimization variables.*

Symbol	Name	Type	Number
y_{ij}	Profile selection	Binary	$\sum_{i=1}^{n_M} n_{Pi}$
N_{ij}^k	Member force	Continuous	$(\sum_{i=1}^{n_M} n_{Pi}) \cdot n_L$
u_ℓ^k	Nodal displacement	Continuous	$n_d \cdot n_L$

Figure 3.2 shows how cross-section selection variable number j of member i corresponds to a profile in profile selection. The vector of cross-section selection binary variables reads as

$$\mathbf{y} = \{y_{11}, y_{12}, \cdots, y_{1n_{P1}}, y_{21}, y_{22}, \cdots, y_{1n_{P2}}, y_{n_M1}, y_{n_M2}, \cdots, y_{n_M n_{Pi}}\} \tag{3.8}$$

Also, a vector of member axial force variables is stated as

$$\mathbf{N}_i^k = \left\{N_{i1}^k, N_{i2}^k, \cdots, N_{in_{Pi}}^k\right\} \tag{3.9}$$

and furthermore

$$\mathbf{u}_i^k = \left\{u_1^k, u_1^k, \cdots, u_{n_d n_P}^k\right\} \tag{3.10}$$

represents a vector of nodal displacement variables.

3.2.2 Constraints Related to Profile Selection Variables

It it obvious, that only one profile is allowed to be selected for a member. Also in practical applications it is common, that unique profiles are assigned for upper and lower chord members, respectively. In the following, these issues have been addressed.

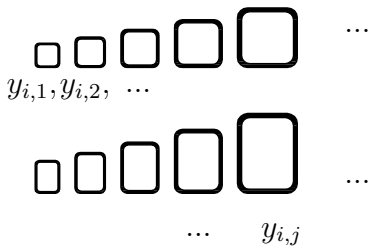

Figure 3.2 *Member profile selection variables.*

Cross-section selection variable constraints

Following constraints, that are related to the cross-section selection variables, ensure that only one profile is selected for member i:

$$\Omega_N = \left\{ \mathbf{x} \,|\, \sum_{j=1}^{n_{Pi}} y_{ij} = 1 \quad \forall\, i \in \mathcal{M} \right\} \tag{3.11}$$

Member grouping constraints

Member grouping enables to assign a unique profile $p_i \in \mathcal{P}_i$ for members $\mathcal{P}_i$ belonging to the same group. If members belong to a group, following constraint must satisfied

$$\Omega_G = \{ \mathbf{x} \,|\, y_{r_1 j} = y_{r_2 j} \quad \forall\, j \in \mathcal{P}, \quad r_1, r_2 \in \mathcal{G} \} \tag{3.12}$$

In Eq. (3.12), members belonging to a group are denoted by $\mathcal{G} \subset \mathcal{M}$.

3.2.3 Nodal Equilibrium

Equilibrium of member forces as well as external loads must prevail in each node of a static structure. This is shown in Figure 3.3. In SAND approach, equilibrium equations are brought into the problem formulation which is showcased in the following.

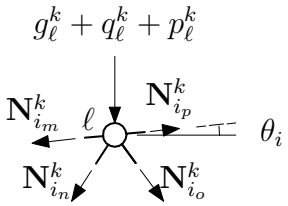

Figure 3.3 *Nodal equilibrium.*

Exact Self Weight

In this study, truss self weight is considered in the equations of equilibrium. As Figure 3.4 shows, equivalent nodal loads are added to the nodes to model the effect

of self weight.

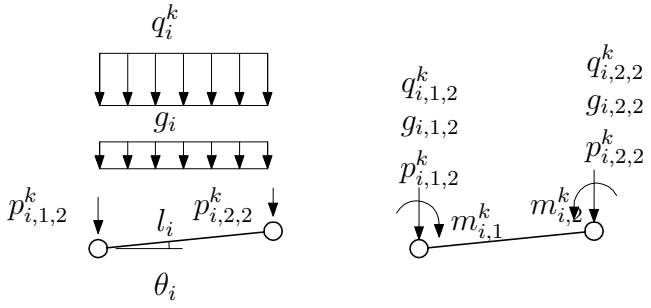

Figure 3.4 *Equivalent nodal loads, y-direction.*

and self weight matrix is formulated by

$$\mathbf{B}_g = \begin{bmatrix} \mathbf{g}_{1,1} \cdots \mathbf{g}_{1,n_{P1}} & \cdots & \mathbf{g}_{n_M,1} \cdots \mathbf{g}_{n_M,n_{Pn_M}} \end{bmatrix} \tag{3.13}$$

Column vector $\mathbf{g}_{i,j} \in \mathbb{R}^{n_d}$ takes into account self weight of profile j of member i. Self weight is added to the rows $d \in \mathcal{D}_{vert}$ of the equilibrium equations, where $\mathcal{D}_{vert}$ denotes vertical displacement degrees of freedom. Also, let d be associated with the node ℓ_d and let member i belong to a group of members $\mathcal{M}_{\ell,d}$ connected to the node ℓ_d. Then, element $d \in \mathcal{D}$ of vector $\mathbf{g}_{i,j}$ is defined as

$$[g_d]_{i,j} = \begin{cases} -\frac{1}{2}\rho \hat{A}_{ij} L_i a_g & \text{, if} \quad d \in \mathcal{D}_{vert} \ \wedge \ i \in \mathcal{M}_{\ell,d} \\ 0 & \text{, otherwise} \end{cases} \tag{3.14}$$

In above, $a_g = 9.81$ m/s^2 represents gravitational acceleration.

Line loading

Equivalent nodal loads, that take into account the effect of transversal line loading acting on profile j of member i, can be expressed as follows

$$q_{i,\ell}^k = \begin{cases} \frac{1}{2} q_i^k L_i \sin\theta_i & \text{(for x-directional load)} \\ \frac{1}{2} q_i^k L_i \cos\theta_i & \text{(for y-directional load)} \end{cases} \quad \forall \quad i \in \mathcal{M}_\ell, \, \ell \in \mathcal{N}, \tag{3.15}$$

Bending moment resulting from transversal line loading must be taken into account. Here, approximation for maximum bending moment is assumed

$$m_{i,\ell} = \frac{1}{10} q_i^k {L_i}^2 \cos^2\theta_i \quad \forall \quad i \in \mathcal{M}_j, \, \ell \in \mathcal{N} \tag{3.16}$$

where $\mathcal{N}$ is structure nodes and $\mathcal{M}_\ell \subset \mathcal{M}$ is members connected to a node ℓ.

Resultant force of equivalent nodal loads associated to a degree of freedom can be calculated by

$$q_d^k = \sum_i q_{i,\ell}^k \quad \forall \quad i \in \mathcal{M}_\ell,\ d \in \mathcal{D}_\ell,\ \ell \in \mathcal{N} \tag{3.17}$$

where $\mathcal{D}_\ell$ is degrees of freedom associated to node ℓ.

Equations of Equilibrium

When the effect of the exact self weight of the truss is implemented into the problem, the equations of equilibrium read as

$$\Omega_{EQ} = \left\{ \left[\mathbf{y}, \mathbf{N}^k, \mathbf{u}\right]^T \mid \begin{bmatrix} \mathbf{B}_g & \mathbf{B} \end{bmatrix} \begin{bmatrix} \mathbf{y} \\ \mathbf{N}^k \end{bmatrix} = \mathbf{p}^k + \mathbf{q}^k, \quad \forall\, k \in \mathcal{L} \right\} \tag{3.18}$$

where $\mathbf{B}_g \in \mathbb{R}^{n_d \times n_Y}$ represents the sub matrix that takes into account the effect of the truss self weight, $\mathbf{B} \in \mathbb{R}^{n_d \times n_Y}$ represents the expanded static matrix that consists of the cosines of the member normal forces.

Let $s \in \{1, 2\}$ denote spatial dimension. Also, let $e \in \{1, 2\}$ represent the member end index. Furthermore, let $d_{i,e,s}$ denote global displacement degree of freedom associated to the end e of member i in the spatial direction s. Let also $\mathbf{b}_{ij}$ be a column of the matrix $\mathbf{B}$. Element number $d \in \mathcal{D}$ of the column $\mathbf{b}_i$ is then formed

$$[b_i]_d = \begin{cases} \ell_i & \text{if } d = d_{i,1,1}, \\ m_i & \text{if } d = d_{i,1,2}, \\ -\ell_i & \text{if } d = d_{i,2,1}, \\ -m_i & \text{if } d = d_{i,2,2}, \\ 0 & \text{otherwise} \end{cases} \tag{3.19}$$

Direction cosines are then calculated by

$$\ell_i = \frac{X_{i12} - X_{i11}}{L_i}, \qquad m_i = \frac{X_{i22} - X_{i21}}{L_i} \tag{3.20}$$

Here, $\mathbf{X}_{i,d,1}$ and $\mathbf{X}_{i,d,1}$ denote nodal coordinates of a member $i \in \mathcal{M}$ ends $k \in \{1, 2\}$ in direction 1 and 2, respectively. Member length is computed by

$$L_i = \sqrt{(X_{i12} - X_{i11})^2 + (X_{i22} - X_{i21})^2} \tag{3.21}$$

Statics matrix can be written as

$$\mathbf{B} = \left[\overbrace{\mathbf{b}_1\ \mathbf{b}_1 \cdots \mathbf{b}_1}^{n_{P1}} \overbrace{\mathbf{b}_2\ \mathbf{b}_2 \cdots \mathbf{b}_2}^{n_{P2}} \quad \cdots \quad \overbrace{\mathbf{b}_{n_M}\ \mathbf{b}_{n_M} \cdots \mathbf{b}_{n_M}}^{n_{Pn_M}} \right] \tag{3.22}$$

where n_{Pi} denotes the number of available profiles for member i.

3.2.4 Member Force constraints

Member force constraints are utilized to enforce the force-displacement relationship as follows

$$\Omega_F = \left\{ \mathbf{x} \,|\, \begin{array}{l} \frac{E_i A_{ij}}{L_i} \mathbf{b}_i^T \mathbf{u}^k - N_{ij} \geq (1 - y_{ij}) \underline{N}_{ij}^k \\ \frac{E_i A_{ij}}{L_i} \mathbf{b}_i^T \mathbf{u}^k - N_{ij} \leq (1 - y_{ij}) \overline{N}_{ij}^k \end{array} \right\} \quad \forall \quad i \in \mathcal{M},\, j \in \mathcal{N},\, k \in \mathcal{L} \tag{3.23}$$

where

$$\underline{N}_{ij}^k = \min_{\underline{\mathbf{u}} \leq \mathbf{u}^k \leq \overline{\mathbf{u}}} \frac{E_i A_{ij}}{L_i} \mathbf{b}_i^T \mathbf{u}^k = \frac{E_i A_{ij}}{L_i} \left(\sum_{r:b_{ir}>0} b_{ir} \underline{u}_r + \sum_{r:b_{ir}<0} b_{ir} \overline{u}_r \right) \tag{3.24}$$

$$\underline{N}_{ij}^k = \max_{\underline{\mathbf{u}} \leq \mathbf{u}^k \leq \overline{\mathbf{u}}} \frac{E_i A_{ij}}{L_i} \mathbf{b}_i^T \mathbf{u}^k = \frac{E_i A_{ij}}{L_i} \left(\sum_{r:b_{ir}>0} b_{ir} \overline{u}_r + \sum_{r:b_{ir}<0} b_{ir} \underline{u}_r \right) \tag{3.25}$$

Note that when profile j for member i is selected, i.e. y_{ij} takes value 1, then corresponding constraint becomes the constitutive law. When y_{ij} takes value 0, then "big" values obtained from Eq. (3.24) ensure, that corresponding constraint remain inactive.

3.2.5 Member Strength and Stability Constraints

Constraints associated with member strength and stability can be stated as follows

$$\Omega_S = \left\{ \mathbf{x} \,|\, \underline{N_{\mathrm{Rd}}}_{ij} \leq N_{ij}^k \leq \overline{N_{\mathrm{Rd}}}_{ij} \quad \forall\, j \in \mathcal{P} \right\} \tag{3.26}$$

where $f_{\mathrm{y},i} A_{ij}$ is substituted to $N_{\mathrm{j,0,Rd}}$ (see Eq. (2.24)) for lower chord members and where

$$\underline{N_{\mathrm{Rd}}}_{ij} = \max \left\{ \underline{N_{\mathrm{Rd}}}_{ij}^k, -f_{\mathrm{y},i} A_{ij}, -\chi_{Mb,ij}^k f_{\mathrm{y},i} A_{ij} \right\} y_{ij} \tag{3.27}$$

$$\overline{N_{\mathrm{Rd}}}_{ij} = \min \left\{ \overline{N_{\mathrm{Rd}}}_{ij}^k, f_{\mathrm{y},i} A_{ij}, \chi_{MN,ij}^k f_{\mathrm{y},i} A_{ij} \right\} y_{ij} \tag{3.28}$$

Term $-\chi_{Mb,ij}$ (see Section 2.7) is resistance reduction factor corresponding to the combined buckling and bending and where $\chi_{MN,ij}$ (see Section 2.6) is resistance reduction factor corresponding to the combined axial force and bending. Eq. (3.26) can be reformulated as

$$\Omega_S = \left\{ \mathbf{x} \,|\, \begin{array}{ll} \frac{N_{\mathrm{Rd}}{}^{k}_{ij}}{} y_{i,j} - N_{i,j} & \leq 0 \\ -\overline{N_{\mathrm{Rd}}}{}^{k}_{ij} y_{i,j} + N_{i,j} & \leq 0 \end{array} \right\}, \quad \forall\, i \in \mathcal{M}\,,\, j \in \mathcal{P} \tag{3.29}$$

3.2.6 Joint Geometry Constraints

Joint geometry constraints guarantee, that width of a brace profile does not exceed straight part of a chord profile. This is enables the welding brace member B and chord member C. For joints to fulfil the conditions given in Section 2.5.3, following constraints are presented:

$$\Omega_{JG} = \left\{ \mathbf{x} \,|\, \begin{array}{rl} 0.35 b_{jC}\, y_{iC,jC} & \leq b_{jB}\, y_{iB,jB} \\ b_{jB}\, y_{iB,jB} & \leq 0.85 b_{iC}\, y_{iC,jC} \end{array} \right\} \tag{3.30}$$

where $b_{iC,jC}$ and $b_{iB,jB}$ refer to profile side lengths of members $i_C \in \mathcal{M}_{C,\ell}$ and $i_B \in \mathcal{M}_{B,\ell}$. In Eq. (3.30), $i_C \in \mathcal{M}_{C,\ell}$, $i_B \in \mathcal{M}_{B,\ell}$, where sets $\mathcal{M}_{C,\ell}$ and $\mathcal{M}_{B,\ell}$ denote chord and brace members connected to node ℓ, respectively. Also, profiles $j_C \in \mathcal{P}_C$, $j_B \in \mathcal{P}_B$.

3.2.7 Objective function

Weight

The mass of the Truss is obtained by

$$W(\mathbf{x}) = \sum_{i=1}^{n_M} \sum_{j=1}^{n_P} \rho_i L_i A_i j y_{ij} \tag{3.31}$$

where $\rho = 7850 \cdot 10^{-9}$ [kg/mm^3] is density of the steel and L_i is the length [mm] of the member i.

3.3 Geometry optimization problem

As stated in Section 3.1, geometry optimization problem can be written as

$$\min_{\Delta\mathbf{X}\in\Omega_{Geom}} \Phi(\Delta\mathbf{X}) \tag{3.32}$$

where $\Phi(\Delta\mathbf{X})$ represents the minimum of the lower level problem i.e. the result of sizing optimization for given $\Delta\mathbf{X}$. Geometry constraints define feasible set Ω_{Geom} for geometry optimization. Ω_{Geom} can be written as

$$\Omega_{Geom} = \begin{cases} \underline{\Delta\mathbf{X}} & \leq \Delta\mathbf{X} \leq \overline{\Delta\mathbf{X}} \\ \mathbf{g}(\Delta\mathbf{X}) & \leq \mathbf{0} \end{cases} \tag{3.33}$$

where $\underline{\Delta\mathbf{X}}$ and $\overline{\Delta\mathbf{X}}$ represent linear lower- and upper bounds, later referred as "box constraints". Furthermore, $\mathbf{g}$ represents nonlinear inequality constraints.

3.3.1 Geometry variables

Geometry optimization problem contains only one type of variables, namely nodal coordinate variation variables, i.e. truss geometry variables. Geometry variables express the nodal variation with respect to the initial geometry. Geometry variable vector can be written as

$$\Delta\mathbf{X} = \begin{cases} \begin{bmatrix} \Delta X_1 & \Delta X_2 & \dots & \Delta X_{n_c} \end{bmatrix}^{\mathrm{T}} & \text{in "horizontal" optimization} \\ \begin{bmatrix} \Delta X_v \end{bmatrix}^{\mathrm{T}} & \text{in "height" optimization} \end{cases} \tag{3.34}$$

where $\Delta X_1, \Delta X_2, \dots, \Delta X_{n_c} \in \mathbb{R}$ refer to degrees of freedom of nodal coordinate variation corresponding to the chord ("horizontal") direction and $\Delta X_v \in \mathbb{R}$ refers to the degree of freedom corresponding to vertical direction. Nodal coordinate variation in "horizontal" and vertical directions are presented in Figure 3.5– 3.6 respectively. If both "horizontal" and "vertical" directions are allowed to vary, then both "horizontal" and "vertical" are included in the geometry variation variables.

Only structures with symmetric topology are considered in this study. Therefore only node coordinates corresponding to the left hand side (or right hand) of the

Table 3.2 *Geometry optimization variables.*

Symbol	Name	Type	Number
ΔX_ℓ	Nodal coordinate variation	Continuous	n_{GV}

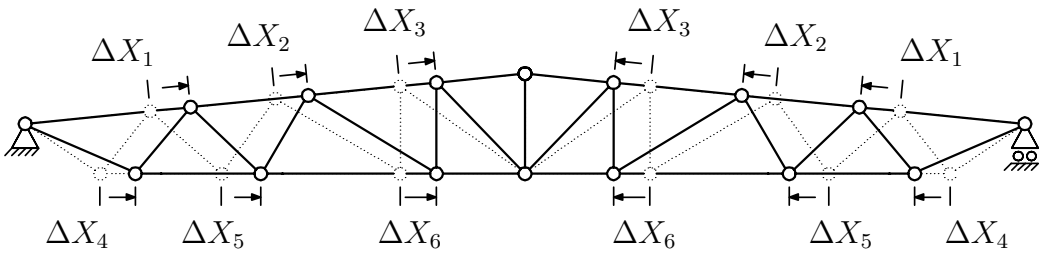

Figure 3.5 *Nodal coordinate displacement "horizontal" variables.*

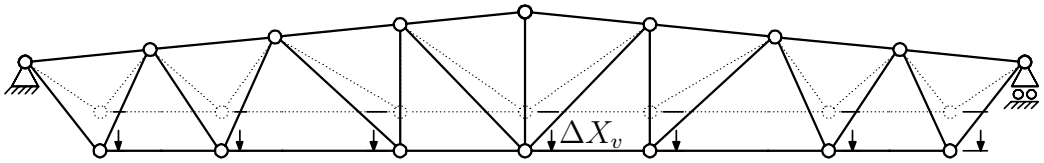

Figure 3.6 *Nodal coordinate displacement "vertical" variables.*

structure need to be considered as variation of the right hand side can be expressed by the variables on the left hand side and vice versa. Also, nodes at the support and nodes at the midspan are kept fixed. Figure 3.5 shows that the number of "horizontal" nodal coordinate variables n_c is equal to the number of nodes on left hand side of the structure excluding the nodes at the midspan and node at the support.

As is shown in Figure 3.6, variation of the truss height is implemented by variation of the nodal coordinates of the lower chord nodes corresponding to the vertical direction. Chord directions are kept fixed throughout the optimization and therefore vertical variation of nodal coordinates is equal. This leads to the number of nodal coordinate variables corresponding to the vertical direction being 1.

In the case of lateral variation, also referred as "horizontal variation", truss height is kept fixed. Consequently, lower chord nodes are only allowed to vary in horizontal direction and vertical degree of freedom of geometry variation is dropped. Similarly, in the case of height variation, lateral positions of the nodes are kept fixed and consequently "horizontal" degrees of freedom of the geometry variation are dropped.

Nodal coordinates of node ℓ, in iteration r with respect to the nodal coordinate variations can be expressed as

$$(X^r_{1,\ell}, X^r_{2,\ell})^T = (X^0_{1,\ell}, X^0_{2,\ell})^T + \mathbf{v}_d \cdot \Delta X^r_\ell, \, \forall \, d \in \mathcal{D}_{GV} \; , \; \ell \in \mathcal{N}_d \tag{3.35}$$

where $(X^0_{1,\ell}, X^0_{2,\ell})$ are the nodal coordinates of the node ℓ in the initial configuration

and ΔX_ℓ^r is the nodal coordinate variation of the node ℓ, in the iteration r. In Eq. (3.35), $\mathbf{v}_d$ indicates the direction vector (Figure 3.7) and $\mathcal{N}_d$ the nodes related to the nodal coordinate variation degree of freedom d. Direction vector $\mathbf{v}_d$ remains constant throughout the optimization process. It can be expressed as

$$\mathbf{v}_i = \cos\theta\ \hat{i} + sin\theta\ \hat{j} \tag{3.36}$$

where θ denotes angle of the geometry variation direction vector.

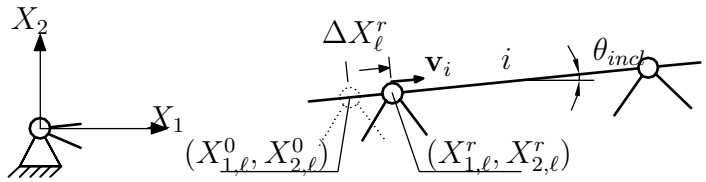

Figure 3.7 *Nodal coordinates with respect to nodal coordinate variation.*

3.3.2 Box Constraints

Box constraints are linear constraints defining the domain of the nodal coordinate variations.

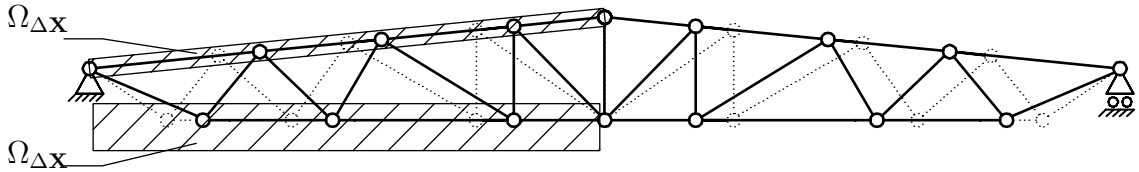

Figure 3.8 *Box constraints.*

As presented in Figure 3.8, coordinate variation of nodes along the chord directions is limited between the ridge and the support. In general form, box constraints read as

$$\Omega_{\Delta\mathbf{X}} = \left\{\underline{\Delta\mathbf{X}} \leq \Delta\mathbf{X} \leq \overline{\Delta\mathbf{X}}\right\} \tag{3.37}$$

More precisely, box constraints can be expressed as

$$\Omega_{\Delta\mathbf{X}} = \left\{ \begin{array}{lll} -\frac{1}{\cos\theta_{incl}} X^0_{\ell,1} \leq \Delta X_\ell \leq \frac{1}{\cos\theta_{incl}} \left(\frac{L}{2} - X^0_{\ell,1}\right) & \text{in "horizontal" variation} \\ H^0 - \frac{L}{6} \leq \Delta X_v \leq H^0 - \frac{L}{16} & \text{in "height" variation} \end{array} \right\} \tag{3.38}$$

where $X^0_{\ell,1}$ is the nodal coordinate variable referring to the node(s) ℓ of the initial geometry ($\mathbf{X}^0$), and where θ_{incl} refers to the inclination angle of the chord the node belongs to, and furthermore L refers to the truss span.

In Eq. (3.38), 2^{rd} row represents constraints corresponding to the height variation (ΔX_v), which is limited according to the minimum and maximum height. H^0 is the height of the initial truss design.

Inclination angle corresponding to the geometry variation degree of freedom can be generally derived from the initial configuration $\Delta\mathbf{X}_0$. where denotation $\mathbf{v}\{d\}(r)$ stands for element $r \in \{1, 2\}$ of the direction vector corresponding to the geometry variation dof $d \in \mathcal{D}_{GV}$

Note, that the box constraints mentioned above do not limit adjacent nodes from "travelling" across each other. This leads to the question of "melting nodes" i.e. coinciding nodal coordinates which result in singular equality matrix and non-solvable problem (Achtziger 2007). Also, arises the question of coinciding members, which leads to the question of creation of new members, joints etc. These problems are however circumvented due to the member angle constraints, as member angle constraints won't allow nodes or members to coincide. This is presented below in section 3.3.3.

3.3.3 Member Angle Constraints

Due to welding requirements angles between adjacent members connected by joint must be equal or greater than 30°. Member angle constraints state as

$$\Omega_\theta = \{\Delta\mathbf{X} \,|\, 30 \leq \theta_{mi1,mi2}(\Delta\mathbf{X}) \,\forall m_{i1}, m_{i2} \in \mathcal{M}_{adj}\} \tag{3.39}$$

where $\theta_{mi1,mi2}$ is angle between members m_{i1} and m_{i1}. Also, $\mathcal{M}_{adj}$ refers to the group of members, that are adjacent and connected by a joint. Figure 3.9 shows members m_{i1} and m_{i1} that are adjacent and connected by common joint (node ℓ). Figure shows also, that symmetry is again exploited as the left hand side angle constraints are only implemented.

Angle $\theta_{i_m i_n}$ in above equation 3.39 can be expressed by

$$\theta_{i_m i_n}(\Delta\mathbf{X}) = \arccos\left(\mathbf{v}^T_{mi1}\mathbf{v}_{mi2}\right) \,\forall\, m_{i1}, m_{i2} \in \mathcal{M}_{adj} \tag{3.40}$$

Note that on the member angle between 1^{st} brace and 1^{st} lower chord member is

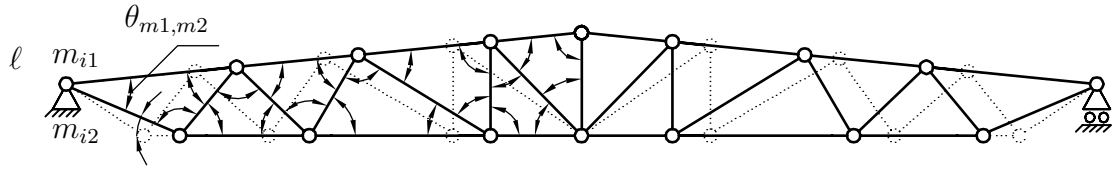

Figure 3.9 *Member angle constraint for member m_{i1} and m_{i2}.*

also limited to over 30° despite members not being adjacent. Therefore constraint is expressed with respect to the angle between members as

$$\Omega_\theta = \{\Delta\mathbf{X} \,|\, 150 \geq \theta_{m_{BR1},m_{LC1}}(\Delta\mathbf{X})\} \tag{3.41}$$

By plugging equation 3.40 into the equations 3.39 and 3.41 yields

$$\mathbf{g} \leq \mathbf{0}, \tag{3.42}$$

where

$$\mathbf{g} = \begin{cases} - & \arccos\left(\mathbf{v}_{m_{i1}}^T \mathbf{v}_{m_{i2}}\right) + 30 \;\forall\; m_{i1}, m_{i2} \in \mathcal{M}_{adj} \\ & \arccos\left(\mathbf{v}_{m_{BR,1}}^T \mathbf{v}_{m_{UC,1}}\right) - 150 \end{cases}.$$

The former row of the Eq. (3.3.3) constitutes the constraint referring to the adjacent members. The latter row constitutes the constraint referring to the joint between 1^{st} brace member $m_{BR,1}$ and 1^{st} lower chord member $m_{UC,1}$, which doesn't form a triangle and therefore are left out of the former constaints.

3.3.4 Objective function

In implicit programming approach, evaluation of geometry variation objective "function" states as

$$\Phi(\Delta\mathbf{X}^r) \tag{3.43}$$

which is in fact evaluation of sizing problem, i.e. global minimizer of sizing optimization problem for truss geometry expressed by nodal coordinate variation $\Delta\mathbf{X}^r$ in iteration r. If there is no solution for the sizing problem for coordinate variation $\Delta\mathbf{X}^r$, then objective function is set

$$\Phi(\Delta\mathbf{X}^r) = \phi_\infty, \tag{3.44}$$

where ϕ_∞ is a "large" number, i.e. larger in the order of magnitude than any possible minimum for the sizing problem. By doing this, as stated previously in section 3.1, geometry variation objective function becomes defined in the whole domain Ω_{Geom} and geometry variation problem solver does not crash when the sizing optimization doesn't have feasible solution. In practice, this can occur when the member actions exceed the resistance of any available profile which leads to sizing problem not being solvable.

4. OPTIMIZATION PROCEDURES

Patience of practicing engineer sets requirements for engineering software. Calculation time turns out to be a pivotal factor for the the design tools to have success among structural engineers. In this chapter, multiple procedures are proposed to decrease the duration of the optimization run. Also, various aspects involved in the optimization procedure are highlighted.

4.1 Procedure overview

Optimization is performed within 5 minutes time frame. Various procedures are needed in order to obtain acceptable results within imposed time limitation. Task is to find an appropriate trade-off between suitable results and calculation time.

General optimization procedure is illustrated in Figure 3.1. Pre and post sizing is performed utilizing full profile selection for each member group. In optimization phase different optimization procedures are employed to hasten the optimization. Table 4.1 shows the procedures utilized in optimization phase.

4.1.1 Procedure A

In procedure A, no limitations are imposed on profile catalog in the optimization phase i.e. the full problem is solved. Therefore, A is a point of comparison for later procedures.

4.1.2 Procedure B

In procedure B, large and small profiles are removed from the profile selection which will reduce the number of binary variables included in the sizing optimization. Below, UC and LC refer to upper and lower chord, respectively. BR refers to braces. Following heuristics are employed to determine which profiles are to be reduced from the profile selection. Reasoning behind heuristics is simple. Truss with maximum

Table 4.1 *tab:General description of optimization approaches.*

A	Chord profiles	Complete catalogue
	Brace profiles	Complete catalogue
B	Chord profiles	Large and small profiles removed
	Brace profiles	Large and small profiles removed
C	Chord profiles	Large and small profiles removed
	Brace profiles	Largest preprocessing profile selected
	Profile size constraints	NOT implemented
D	Chord profiles	Large and small profiles removed
	Brace profiles	17 profiles selected

height has minimum axial member forces in chords whereas truss with minimum height has maximum axial forces in chords.

First truss, denoted by T_{max}, is a truss with vertical geometry variable ΔX_v equal to the value, that produces "the tallest" truss (see Figure 3.8). Second truss, denoted by T_{min} is a truss with ΔX_v equal to the value, that produces "the lowest" truss. Then pre sizing is performed to obtain T_{max} and T_{min}. Smallest chord profile A_j of T_{max} is extracted. Due to inaccuracy of the procedure, A_j is multiplied by factor 0.9 to obtain a lower bound for chord cross-section areas

$$\underline{A} = 0.9A_j. \tag{4.1}$$

Following similar reasoning, maximum cross-section area A_j is extracted from truss T_{min}. Now, upper bound for chord cross-section areas is obtained by setting

$$\overline{A} = 1.3A_j. \tag{4.2}$$

Note that relatively greater correction factor is used when determining the upper bound. Then, profiles selection for chords is selected by setting

$$\{j \in \mathcal{P}_{CH} \mid \underline{A} \leq A_j \leq \overline{A}\} \tag{4.3}$$

Note that presented heuristics only apply to trusses with equal upper chord and equal lower chord profiles. Also, steel grade must be equal for all chord members. Now, only brace profiles j are selected, that fulfil the condition

$$\{j \in \mathcal{P}_{BR} \mid 0.3b_{CH,min} \leq b_j \leq 0.85b_{CH,max}\}, \tag{4.4}$$

where $b_{CH,min}$ is the minimum and $b_{CH,max}$ is maximum chord side length found among chord profiles $\mathcal{P}_{CH}$.

4.1.3 Procedure C

In procedure C, a truss with minimum initial height T_{min} is obtained as described in *Section* 4.1.2 by pre sizing. Let $\mathcal{P}_{BR,T} \subset \mathcal{P}_{BR}$ denote brace profiles of T_{min}. Then, in the optimization phase, brace profile j with the maximum cross-section area

$$\{j \mid \max_{j \in \mathcal{P}_{BR,T}} A_j\} \tag{4.5}$$

is assigned to all brace members $i \in \mathcal{M}_{BR}$. Note that profile size constraints are removed from the optimization to ensure, that unnecessarily big upper or lower chord profiles are not enforced. Note also, that optimization problem is changed drastically. This is highlighted later in numerical calculations.

4.1.4 Procedure D

In procedure D, subset of chord profiles $\mathcal{P}_{CH,B} \subset \mathcal{P}_{CH}$ and brace profiles $\mathcal{P}_{BR,B} \subset \mathcal{P}_{BR}$ are chosen according to procedure B. Then 17 profiles are selected systematically from the brace profiles $\mathcal{P}_{BR,B}$ according to following procedure. Assume n_{PBR} denotes the number of brace profiles. Then a set of 17 real numbers are chosen systematically from interval between 1 and n_{PBR} by

$$\mathcal{P}_{BR,R} = \{1 + 0 \cdot \delta, 1 + 1 \cdot \delta, \cdots, 1 + 16 \cdot \delta\} \tag{4.6}$$

where increment $\delta \in \mathbb{R}$ is defined as

$$\delta = \frac{n_{PBR}}{16} \tag{4.7}$$

Furthermore, each real-valued number $r \in \mathcal{P}_{BR,R}$ rounded to nearest integer i which is included in the set of reduced profiles by setting

$$\mathcal{P}_{BR,D} = \{i \bigcup \mathcal{P}_{BR,D}\} \tag{4.8}$$

It is important to make sure, that in same profile cannot be selected twice.

5. NUMERICAL CALCULATIONS

Proposed approach for the geometry optimization and optimization procedures are demonstrated on numerous examples. First, objective function is investigated to gain knowledge for the geometry variation (Eq. (3.32)). Also, algorithms used in geometry optimization are compared with each other. Robustness of the algorithms is studied and time consumption of the computing. Then, optimization procedures are compared with each other. Lastly, examples are studied thoroughly to illustrate the changes that take place in geometry optimization.

In each example, density of the material $\rho = 7850\text{kg/m}^3$ and elastic modulus $E = 210000$ MPa. Member profiles are square hollow section (SHS) selected from the catalog of the steel manufacturer SSAB (2017). Profile data is given in Appendix A. According to buckling constraints of Eurocode 3, buckling imperfection factor $\alpha = 0.49$ for cold formed hollow sections. Also, partial safety factors $\gamma_{\text{M0}} = 1.0$ and $\gamma_{\text{M1}} = 1.0$. Support moment is considered according to Eq. (2.34). Eccentricity of the support reaction is assumed $e = 150$ mm Also, when high strength steel is assigned to lower chord, lower chord resistance for axial tension is calculated using Eq. (2.24).

5.1 Solvers

Three solvers were considered in this study. The mixed variable truss sizing problem in each example is solved by the software Gurobi 7.0.2 (Gurobi Optimization, Inc. 2017). The relative optimality gap is set to 0.1%. This is the relative difference between the best known solution and the lower bound obtained from the relaxations. Thus, the solutions obtained are global optima within the stated numerical accuracy.

In procedural study, heuristic direct search algorithm Matlab Patternsearch (MathWorks, Inc. 2017) is tested for the upper lever problem solving. Patternsearch implements a minimal and maximal positive basis search pattern. It is suitable for discontinuous, nonlinear and nonconvex problem solving (MathWorks, Inc. 2017). Convergence tolerance for objective function absolute value of change is set to 0.1. Convergence tolerance for norm of geometry variable vector as well as mesh tolerance

are set to 0.0001. Here, mesh tolerance is the step size of last iteration.

Also gradient based interior point algorithm MathWorks, Inc. (2017) algorithm is experimented on the upper level problem solving using default settings.

Examples in procedural study were computed by cluster where parallel computing were utilized in geometry optimization. Per task, 16 cpus and 24576 megabytes of memory per cpu were allocated.

5.2 1-D cases

In implicit programming approach, selection of geometry optimization algorithm must be done considering carefully the nature of the problem in hand. Therefore two example cases are studied to provide information about the behaviour of the objective function. Cases were selected to be one dimensional for them to be illustrative. Truss height is perhaps the most crucial geometric design parameter. Therefore height variation was selected to be one case (see Figure 5.1). On the other hand some information about the effect of lateral node variation was also needed. Thus, second case was selected as shown in Figure 5.3.

Table 5.1 *Design parameters for 1-D cases.*

Span	20000 mm
Type/Division	K/4
Loadcase(1)	line loading 25.0 $\frac{\text{kN}}{\text{m}}$
Roofslope	1/ 20
grades $\{UC, LC, BR\}$	$\{S700, S700, S420\}$

The study of design space was performed using design parameters described in Table 5.1. Objective function "curves" were obtained by performing sizing optimization in uniform intervals. The density of the interval was determined considering on the one hand "adequate" accuracy of the information, and on the other hand "reasonable" limits of the computing time. The interval was set to be approximately 2 mm.

In the following, nature of objective function as well as applicable solvers for upper level are investigated. Objective function landscape is discovered to be "rugged" i.e. piecewise continuous. This is highlighted on Figure 5.2 and Figure 5.4. Discontinuities are caused by discrete cross-section profile selection, which can be observed by examining the resulting designs on both sides of the discontinuous points.

In continuous intervals, gradient of the objective function is determined by the geometric variation of structure with fixed profiles. Thus, the negative gradient

Table 5.2 *Constraints for the 1-D cases.*

Member strength constaints	Implemented
Member stability constraints	Implemented
Compatibility constraints	Implemented
Joint strength constraints	NOT implemented
Member angle constraints	$\theta_{ij} \geq 30°$
Profile size constraints	$\frac{b_i}{b_0} \in [0.35, 0.85]$
Self weight	Implemented
Box constraints	Chord direction: $\mathbf{X}_{hor} \in [0, L]$, Vertical direction: $\mathbf{X}_{vert} \in \left[\frac{L}{15}, \frac{L}{5}\right]$
Loading cases	1

direction is not necessarily equal to the direction of the global minimum. Example cases show also, that the objective functions have single valued solution in their geometric domain, which is a premise in implicit programming approach (Achtziger 2007).

5.2.1 Height Variation

In height variation the changes in brace member lengths dominate the changes in objective function in continuous intervals. In discontinuous points profiles change.

Height variation is started from 7 different heights, denoted by a, b, c, d, e, f and g, utilizing interior point algorithm (MathWorks, Inc. 2017). On the right hand side of the global minimum negative of the gradient is pointing towards the global minimum, whereas on the left hand side the gradient is pointing away from the minimum. Consequently, as can be seen in Figure 5.2, only d, e and g located on the right hand side of the minimum succeed in finding the global minimum. None of the points located at the left hand side of the global minimum proceed towards the minimum. Success of gradient based algorithm is strongly depending on "good" starting point. According to optimization theory, gradient based algorithms are not suitable for solving of discontinuous problems. This is apparent according to the results of height variation as well.

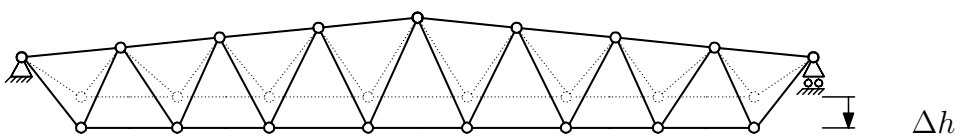

Figure 5.1 *Variation of truss height.*

When utilizing pattern search algorithm (MathWorks, Inc. 2017) for the height optimization problem, the global minimum is reached from all starting points. This is a strong indication, that one may resort to heuristic algorithms.

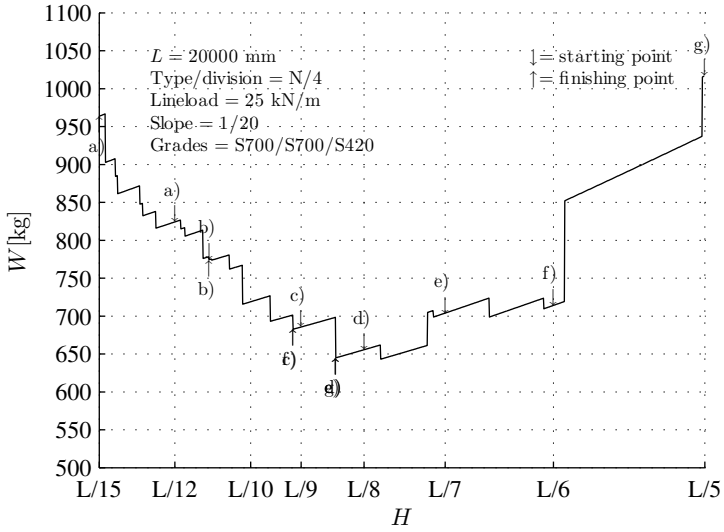

Figure 5.2 *Objective function study, variation of height, interior point algorithm.*

5.2.2 Lateral Variation

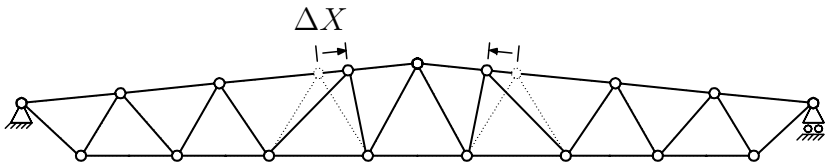

Figure 5.3 *1D lateral variation.*

When varying nodal point of the truss upper chord shown in Figure 5.3, the change in brace member length is again dominating the change in the truss weight. Here, the global optimum is located near the starting point. In this very limited case, the shorter length of compressed member does not "automatically" lead to better objective value.

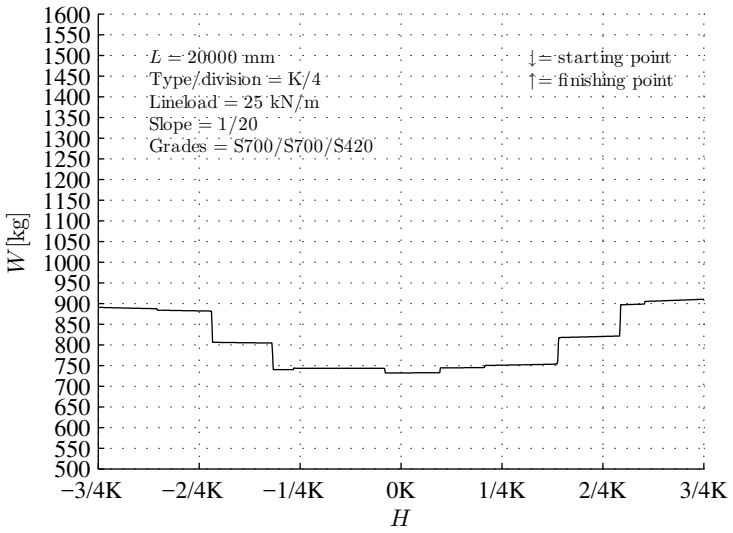

Figure 5.4 *Objective function of lateral variation, free brace profile selection.*

5.3 Multidimensional cases

Here calculations utilizing procedures A, B, C and D (see Section 4) are demonstrated on a set of 108 roof truss cases for each procedure. Design parameters for the cases include truss *span*, line loading q_{Ed}, truss *type*, upper chord *division*, which refers to number of upper chord segments and steel *grades*. Parameters are shown below.

- $span = \{16, 24, 32, 40\}$ [m]
- $q_{Ed} = \{12, 22, 32\}$ [kN/m]
- $type = \{K\}$
- $division = \{3, 4, 5\}$
- $grades = \{S420, S420, S420\}, \{S550, S550, S420\}, \{S700, S700, S420\}$

Truss *span* is selected to represent a wide variety of possible roof truss spans in practical design applications. Line loadings represent "typical" values for Central and Northern European climate conditions. Truss type is selected to be a "commonly used" type. Divisions are also selected to represent a wide variety of possible divisions. In steel grades the usage of high strength steel is investigated.

In Table 5.3 implemented constraints are shown. Displacement constraints are intentionally set very "loose" for them to remain inactive in the optimization. Typically, maximum nodal displacements are around $L/160$ in these cases located at the

mid span. Note again, that joint strength constraints are not fully implemented in the problem. Self weight is considered in exact manner. Box constraints are also set "loose". Possible nodal positions are restricted horizontally between support and the ridge. Vertical constraint is not needed since nodes follow the chord directions.

Table 5.3 *Constraints in multidimensional cases.*

Member strength constaints	Implemented
Member stability constraints	Implemented
Compatibility constraints	$\mathbf{X}_{vert} \leq \frac{L}{50}$
Joint strength constraints	NOT implemented
Member angle constraints	$\theta_{ij} \geq 30°$
Profile size constraints	$\frac{b_i}{b_0} \in [0.35, 0.85]$
Self weight	Implemented
Box constraints	Chord direction: $\mathbf{X}_{hor} \in [0, L]$ Vertical direction: $\mathbf{X}_{vert} = \frac{L}{10}$

In all cases, geometry variation type is "horizontal" variation demonstrated in Figure 3.5. In horizontal variation the height of the truss is fixed. Nodal coordinates are allowed to move along the chord directions. Node positions of the support nodes and the nodes at the ridge are fixed.

5.3.1 Calculation time

Some consideration must be given to the relation between problem size and calculation time. Figure 5.5 shows the correlation between calculation with respect to the number of evaluations and number of sizing variables in procedure A and procedure B. The results presented here are final results, i.e. calculation were run to the global optimum.

It is obvious, that higher number of variables and evaluations will lead to minimal decrease of weight in 5 min results. Number of variables cannot exceed approximately 4000, and number of evaluations must stay below 1000 for algorithm to have a chance to obtain significant decrease in objective function value in 5 minutes. It is also obvious, that optimization will unlikely reach the stopping criteria in 5 minutes. However, in practical engineering, instead of seeking "the best" results, the goal is rather to obtain "a better" result. This is the goal in this thesis as well.

Dividing the total calculation time by the number of evaluations yields time per evaluation. Figure 5.6 shows again, that given the utilized implementation and hardware, number of variables should remain within around 4000. The correlation

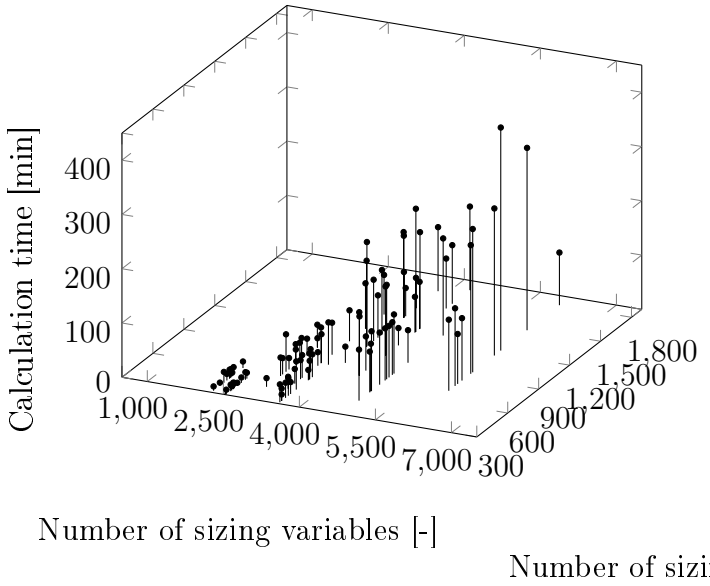

(a) Procedure A.

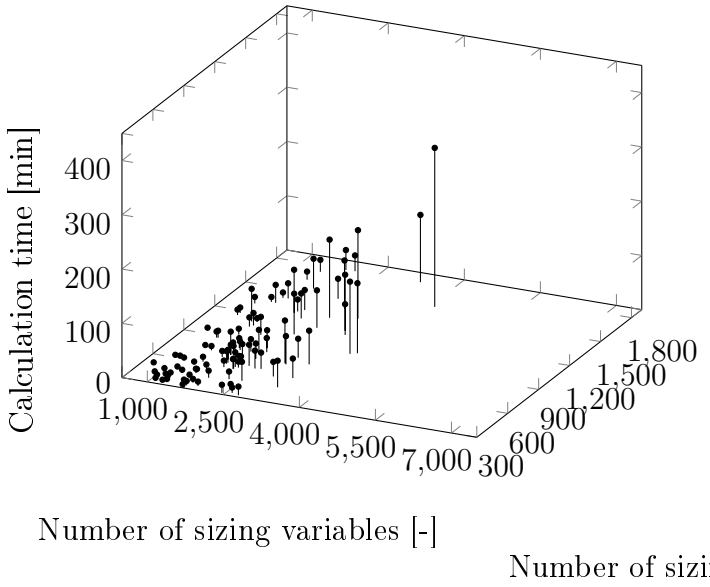

(b) Procedure B.

Figure 5.5 *Calculation time with respect to the number of sizing variables and number of sizing evaluations, horizontal variation.*

between number of sizing variables and calculation time is evident, although the results are more spread with higher number of variables.

5.3.2 Quick results

In the following, best optimization result is picked from each of 9 combinations of 3 line loading and 3 truss span alternatives. Results are presented in Tables 5.4– 5.7 for procedures A, B, C and D, respectively. Considering the goal of the study, namely

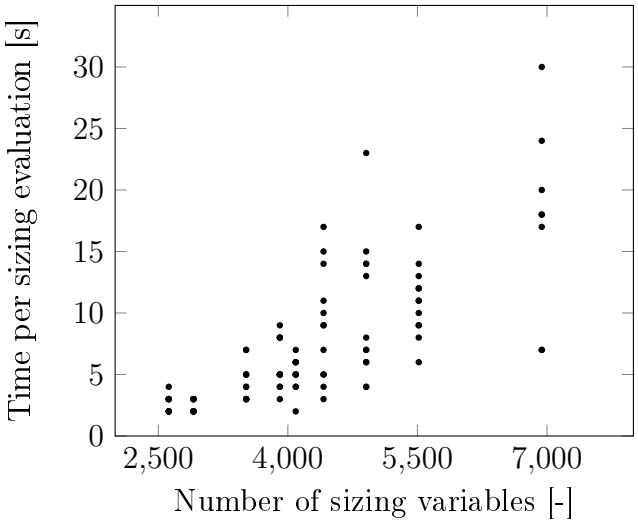

Figure 5.6 *Approach A, calculation time per sizing evaluation with respect to the number of sizing variables, horizontal variation,* $H = \frac{L}{10}$*, type K.*

obtain "good" solution in acceptable time, the resulting weight $W_{Post,5}$ is picked from the 5 minute point of calculations. The final result is naturally considered in case the calculation ended due to fulfilled stopping criteria in less than 5 minutes. In tables, W_{Init} denotes the weight of the initial structure, where as Δp denotes percentual change of the truss weight and ΔW change in kg. Notice, that Δp and ΔW are calculated utilizing pre sizing and post sizing. Total calculation *time* and *division* of the upper chord half are also presented for the best solution.

A closer look at the weight reduction is taken. Best results for procedure A are shown in Table 5.4. Several interesting observations can be made from the results. Procedure provides good results when the span is short. With a combination of a span of 16 m and line loading of 12 $-$22 kN/m the best weight difference percentages are 10.0$-$13.9%. With intermediate to long spans the results drop drastically. With span longer than 24 m or loading more than 22 kN/m the results for procedure A are poor with no weight reduction. Exception is the result with 12 kN/m with a 40 m span with the weight decrease of 11.6%. It is easy to see, that increasing the span and the loading increases calculation time. There might be several reasons for this. One might be that selected set of cases, for a truss with a long span and half span divided in only 3, 4 or 5 segments, leads to unnecessary long compressed chord member lengths. This may lead to narrower domain of the objective function and make it therefore more difficult for geometry optimization algorithm to find a better solution.

Procedure B provides generally better results (see Table 5.5) in all span and loading combinations than procedure A yet the results deteriorate for combinations of span

Table 5.4 *Full problem A, best weight optima.*

L [m]	q [kN/m]	12	22	36
16	W_{Init} [kg]	312	449	575
	$W_{Post,5}$ [kg]	268	404	566
	Δp[%]	-13.9	-10.0	-1.7
	ΔW[kg]	-43	-45	-10
	time [min]	52	30	42
	grades	S700/S700/S420	S700/S700/S420	S700/S700/S420
	division	5	5	4
24	W_{Init} [kg]	665	930	1286
	$W_{Post,5}$ [kg]	645	895	1286
	Δp[%]	-3.1	-3.7	-0.0
	ΔW[kg]	-20	-35	-0
	time [min]	108	118	158
	grades	S550/S550/S420	S700/S700/S420	S700/S700/S420
	division	5	5	5
32	W_{Init} [kg]	1241	1869	2381
	$W_{Post,5}$ [kg]	1199	1860	2368
	Δp[%]	-3.3	-0.5	-0.5
	ΔW[kg]	-42	-10	-12
	time [min]	78	127	113
	grades	S700/S700/S420	S550/S550/S420	S700/S700/S420
	division	5	5	5
40	W_{Init} [kg]	2116	2879	4169
	$W_{Post,5}$ [kg]	1870	2879	4169
	Δp[%]	-11.6	0.0	0.0
	ΔW[kg]	-246	0	0
	time [min]	119	158	192
	grades	S700/S700/S420	S700/S700/S420	S700/S700/S420
	division	5	5	5

over 24 m and loading over 22 kN/m when calculation is stopped after 5 minutes. With span being 16 m or load being 12 kN/m the percentage of weight decrease is up to 15.6 %. Then with the span over 24 m, the the percentage of weight decrease becomes smaller. For example, with the combination of 22 kN/m loading and 32 m span, relative weight decrease is 1.6 %.

Procedure C, shown in Table 5.6, turns out to be the weakest of all proposed procedures with in most cases weight increasing. Reasons behind this behaviour are discussed in greater detail later in Section 5.3.3. It can be stated, that procedure is not applicable in any span or loading scenario utilized in these cases.

Of all the procedures, D provides most consistent relative weight reduction over all span and loading combinations. This is shown in Table 5.7. Even for combinations

Table 5.5 *Procedure B, best weight optima.*

L [m]	q [kN/m]	12	22	36
16	W_{Init} [kg]	312	449	575
	$W_{Post,5}$ [kg]	266	390	561
	Δp[%]	-14.8	-13.1	-2.4
	ΔW[kg]	-46	-59	-14
	time [min]	13	10	15
	grades	S700/S700/S420	S700/S700/S420	S700/S700/S420
	division	5	5	4
24	W_{Init} [kg]	681	930	1286
	$W_{Post,5}$ [kg]	575	879	1259
	Δp[%]	-15.6	-5.5	-2.1
	ΔW[kg]	-106	-51	-27
	time [min]	9	24	76
	grades	S700/S700/S420	S700/S700/S420	S700/S700/S420
	division	5	5	5
32	W_{Init} [kg]	1241	1869	2381
	$W_{Post,5}$ [kg]	1151	1840	2317
	Δp[%]	-7.2	-1.6	-2.7
	ΔW[kg]	-90	-30	-63
	time [min]	20	27	68
	grades	S700/S700/S420	S550/S550/S420	S700/S700/S420
	division	5	5	5
40	W_{Init} [kg]	2116	2879	4169
	$W_{Post,5}$ [kg]	1834	2771	4094
	Δp[%]	-13.3	-3.7	-1.8
	ΔW[kg]	-282	-108	-74
	time [min]	29	104	112
	grades	S700/S700/S420	S700/S700/S420	S700/S700/S420
	division	5	5	5

of span over 24 m and line loading over 22 kN/m, the weight decrease is from 4.3 % to 6.3 %. Therefore it appears, that in procedures A and B, big number of variables played bigger role in increasing the calculation time than chosen set of example cases.

Results from all procedures are combined in Table 5.8. In each box the best result from each load and span combination is presented. Approaches B and D produce highest relative weight decrease in each of 9 loading and span combinations. Especially with the combination of intermediate to long span and loading, procedure D appears to produce the best results. Although it should be mentioned, that with the longest span of 40 m and heaviest line loading of 36 kN/m, the best weight reduction percentage is only 2.4%.

Table 5.6 *Procedure C, best weight optima.*

L [m]	q [kN/m]	12	22	36
16	W_{Init} [kg]	301	449	575
	$W_{Post,5}$ [kg]	314	435	622
	Δp[%]	4.1	-3.2	8.2
	ΔW[kg]	12	-14	47
	time [min]	1	2	1
	grades	S700/S700/S420	S700/S700/S420	S700/S700/S420
	division	4	5	4
24	W_{Init} [kg]	681	930	1286
	$W_{Post,5}$ [kg]	723	970	1286
	Δp[%]	6.1	4.4	0.0
	ΔW[kg]	42	40	0
	time [min]	2	1	1
	grades	S700/S700/S420	S700/S700/S420	S700/S700/S420
	division	5	5	5
32	W_{Init} [kg]	1342	1945	2381
	$W_{Post,5}$ [kg]	1254	1945	2381
	Δp[%]	-6.5	0.0	0.0
	ΔW[kg]	-88	0	0
	time [min]	3	2	1
	grades	S550/S550/S420	S700/S700/S420	S700/S700/S420
	division	5	5	5
40	W_{Init} [kg]	2074	2879	-
	$W_{Post,5}$ [kg]	1992	2879	-
	Δp[%]	-4.0	0.0	-
	ΔW[kg]	-83	0	-
	time [min]	3	2	-
	grades	S550/S550/S420	S700/S700/S420	- / - / -
	division	5	5	-

It is obvious that stronger steel grades produce best results in weight optimization. In most of the cases, combination grade S700 for the chords and grade S420 for the braces offer smallest weight in studied combinations. Also, dense upper chord division provides good results in weight optimization.

In calculations, that are stopped at early stage, one might make a presumption, that smaller problems would converge much faster and therefore benefit in results taken on the 5 minutes point. However, by observing the results one can see, that this is not the case. Result seem to proof quite the contrary. In most cases the division of 5 gives the best solution.

In Table 5.9 average weight differences as well as medians are provided for all procedures. Here, solutions for the procedure A are final results to provide "good"

Table 5.7 *Procedure D, best weight optima.*

L [m]	q [kN/m]	12	22	36
16	W_{Init} [kg]	312	449	575
	$W_{Post,5}$ [kg]	266	390	562
	Δp[%]	-14.8	-13.1	-2.2
	ΔW[kg]	-46	-59	-13
	time [min]	12	10	6
	grades	S700/S700/S420	S700/S700/S420	S700/S700/S420
	division	5	5	4
24	W_{Init} [kg]	681	930	1286
	$W_{Post,5}$ [kg]	575	892	1261
	Δp[%]	-15.6	-4.1	-1.9
	ΔW[kg]	-106	-38	-25
	time [min]	9	9	48
	grades	S700/S700/S420	S700/S700/S420	S700/S700/S420
	division	5	5	5
32	W_{Init} [kg]	1241	1869	2381
	$W_{Post,5}$ [kg]	1162	1784	2278
	Δp[%]	-6.4	-4.6	-4.3
	ΔW[kg]	-79	-85	-102
	time [min]	12	22	10
	grades	S700/S700/S420	S550/S550/S420	S700/S700/S420
	division	5	5	5
40	W_{Init} [kg]	2116	2879	4169
	$W_{Post,5}$ [kg]	1835	2681	3905
	Δp[%]	-13.3	-6.9	-6.3
	ΔW[kg]	-281	-198	-264
	time [min]	22	13	23
	grades	S700/S700/S420	S700/S700/S420	S700/S700/S420
	division	5	5	5

reference values. Consequently, 5 minutes result of procedure A are dropped from the final scrutiny. The results for procedures B, C and D are again combined from the solutions taken from the 5 minutes calculations.

By observing Table 5.9 it can be stated, that the solutions for procedure D, with the average weight reduction percentage of 7.5%, provide the best results from all considered optimization procedures in this study. However, average weight reduction percentage for procedure B is only 0.4% lower than for D. This confirms the observation, that procedures D and B are clearly more efficient than A or C.

Table 5.8 *Best results from cases A, B, C and D.*

L [m]	q [kN/m]	12	22	36
16	W_{Init} [kg]	311.8	449.3	575.1
	$W_{Post,5}$ [kg]	265.6	390.3	561.2
	Df [%]	-14.9	-13.2	-2.6
	Df [kg]	-46.2	-59.0	-13.8
	grades	S700/S700/S420	S700/S700/S420	S700/S700/S420
	division	5	5	4
	Appr.	B	D	B
24	W_{Init} [kg]	681.2	930.0	1286.0
	$W_{Post,5}$ [kg]	574.9	878.9	1259.5
	Df [%]	-15.7	-5.7	-3.1
	Df [kg]	-106.3	-51.0	-26.6
	grades	S700/S700/S420	S700/S700/S420	S700/S700/S420
	division	5	5	5
	Appr.	D	B	B
32	W_{Init} [kg]	1241.0	1869.5	2380.7
	$W_{Post,5}$ [kg]	1151.4	1784.2	2278.5
	Df [%]	-7.3	-4.8	-3.5
	Df [kg]	-89.6	-85.2	-102.2
	grades	S700/S700/S420	S550/S550/S420	S700/S700/S420
	division	5	5	5
	Appr.	B	D	D
40	W_{Init} [kg]	2115.9	2879.2	4168.6
	$W_{Post,5}$ [kg]	1834.1	2680.9	3905.0
	Df [%]	-14.5	-7.2	-2.4
	Df [kg]	-281.8	-198.4	-263.6
	grades	S700/S700/S420	S700/S700/S420	S700/S700/S420
	division	5	5	5
	Appr.	B	D	D

Table 5.9 *Results averages and medians, horizontal optimization, approaches A, B, C and D.*

	A	B	C	D
average improvement [kg]	-168	-127	-15	-146
median improvement [kg]	-99	-66	0	-90
average improvement [%]	-8.4	-7.1	-0.7	-7.5
median improvement [%]	-7.1	-5.8	0.0	-6.1

5.3.3 Detailed case

A case with a loading of 22 kN/m and a span of 24 m is taken into closer examination. Stee grade combination is S700 for chords and 420 for braces, respectively. Case is computed utilizing procedures A, B, C and D to the geometry solver convergence criteria. Then changes in the geometry and design are studied closely.

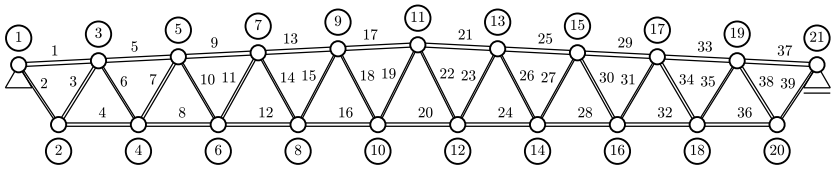

Figure 5.7 *Initial design, $W^* = 930$ kg.*

Table 5.10 *Initial design, utilization ratios.*

Member	Profile	W [kg]	$U_{t,S}$ [%]	$U_{t,B}$ [%]
1, 37	120 × 5.0	42.2	18.40	56.85
2, 39	60 × 3.0	11.2	97.50	-
3, 38	80 × 4.0	20.9	53.89	93.99
4, 36	100 × 4.0	28.2	34.77	-
5, 33	120 × 5.0	42.2	29.36	55.32
6, 35	50 × 3.0	9.6	83.72	-
7, 34	80 × 3.0	16.7	49.59	89.04
8, 32	100 × 4.0	28.2	58.17	-
9, 29	120 × 5.0	42.2	40.97	77.20
10, 31	50 × 3.0	10.0	51.99	-
11, 30	70 × 3.0	15.1	35.67	79.24
12, 28	100 × 4.0	28.2	72.11	-
13, 25	120 × 5.0	42.2	47.14	88.83
14, 27	50 × 3.0	10.5	23.15	-
15, 26	50 × 3.0	10.9	23.08	93.04
16, 24	100 × 4.0	28.2	78.08	-
17, 21	120 × 5.0	42.2	48.70	91.77
18, 23	50 × 3.0	10.9	3.41	13.73
19, 22	50 × 3.0	11.4	3.15	-
20	100 × 4.0	28.2	77.27	-

Here, upper chord half of the considered truss is divided into 5 segments of equal length shown in Figure 5.7. The structure consists of 39 members and 21 nodes.

Initial design is a result of pre sizing, whereas optimum design is a result of post sizing. The initial and optimum designs are illustrated in Figure 5.7– 5.11. Profiles, member weights W, as well as utilization ratios of cross-section resistance $U_{t,S}$ and buckling resistance $U_{t,B}$ are presented in Table 5.10 representing the initial design. Designs obtained by procedures A, B, C and D are shown in Tables 5.11– 5.14. Initial and optimum node coordinates can be observed in Appendix B.

Generally, upper chord members are subjected to bending moment and shear force due to transversal line loading. Also, upper chord members are subject to axial compression. Hence, critical design constraint for the upper chord members is combined buckling and bending presented in Eq. (2.29). Lower chord members are subjected

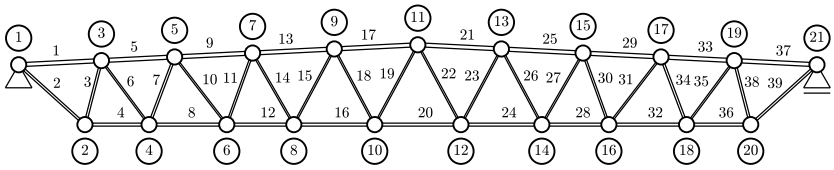

Figure 5.8 *Approach A, $W^* = 877$ kg.*

Table 5.11 *Procedure A, utilization ratios.*

Member	Profile	W [kg]	$U_{t,S}$ [%]	$U_{t,B}$ [%]
1, 37	120 × 5.0	43.7	29.83	96.40
2, 39	70 × 3.0	16.5	100.00	-
3, 38	70 × 4.0	15.8	53.34	94.17
4, 36	90 × 4.0	20.2	40.14	-
5, 33	120 × 5.0	38.7	30.59	51.83
6, 35	50 × 3.0	10.2	88.02	-
7, 34	70 × 3.0	13.3	52.40	99.86
8, 32	90 × 4.0	24.5	64.23	-
9, 29	120 × 5.0	41.2	41.67	76.14
10, 31	50 × 3.0	10.9	57.99	-
11, 30	60 × 3.0	11.9	40.11	99.93
12, 28	90 × 4.0	21.1	80.04	-
13, 25	120 × 5.0	43.2	47.33	92.06
14, 27	50 × 3.0	10.5	25.00	-
15, 26	50 × 3.0	10.9	24.76	99.95
16, 24	90 × 4.0	25.5	87.38	-
17, 21	120 × 5.0	44.1	49.52	99.48
18, 23	50 × 3.0	10.9	2.80	11.32
19, 22	50 × 3.0	11.6	2.60	-
20	90 × 4.0	27.2	86.60	-

to axial tension and therefore critical design constraint is cross-section resistance shown in Eq. (2.25). Due to truss type, brace member are subjected to alternate axial tension and compression so that member nearest to the support is in all cases subjected to axial tension.

In all designs, outermost lower chord node moves towards the ridge thus shortening the lower chord. This represent the most significant change in all geometries. Also for all designs, the lower chord profile changes from 100×4.0 to 90×4.0. For design A and B, the lower chord weight reduces 44 kg where as for C and D the reduction is 45 and 49 kg, respectively. It is worth noting that, in all designs apart from C, upper chord profile and obviously length remain the same resulting in no change in weight. Notice, that the brace member side length of 70 mm does not allow selection of smaller lower chord side length than 90 mm due to joint geometry constraints of Eq. (3.30). Therefore the highest lower chord utility ratio is approximately 87%.

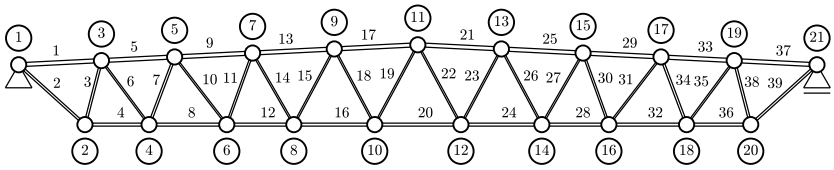

Figure 5.9 *Approach B, $W^* = 877$ kg.*

Table 5.12 *Approach B design, utilization ratios.*

Member	Profile	W [kg]	$U_{t,S}$ [%]	$U_{t,B}$ [%]
1, 37	120 × 5.0	43.7	29.83	96.40
2, 39	70 × 3.0	16.5	100.00	-
3, 38	70 × 4.0	15.8	53.34	94.17
4, 36	90 × 4.0	20.2	40.14	-
5, 33	120 × 5.0	38.7	30.59	51.83
6, 35	50 × 3.0	10.2	88.02	-
7, 34	70 × 3.0	13.3	52.40	99.86
8, 32	90 × 4.0	24.5	64.23	-
9, 29	120 × 5.0	41.2	41.67	76.14
10, 31	50 × 3.0	10.9	57.99	-
11, 30	60 × 3.0	11.9	40.11	99.93
12, 28	90 × 4.0	21.1	80.04	-
13, 25	120 × 5.0	43.2	47.33	92.06
14, 27	50 × 3.0	10.5	25.00	-
15, 26	50 × 3.0	10.9	24.76	99.95
16, 24	90 × 4.0	25.5	87.38	-
17, 21	120 × 5.0	44.1	49.52	99.48
18, 23	50 × 3.0	10.9	2.80	11.32
19, 22	50 × 3.0	11.6	2.60	-
20	90 × 4.0	27.2	86.60	-

Brace member weights are reduced 10 kg in designs A and B. This is due to contraction of compressed members. This results in increased member buckling strength, which enables selecting smaller profiles. In designs C and D, the weight of the brace members increases by 10 kg and 17 kg, respectively. Generally this is partly because of increased profiles, but mostly because of lengthening of compressed members. Also, in design D, sparse profile selection causes more sudden changes in profiles.

Total weight of the trusses is reduced by 53 kg for designs A and B, and 31 kg for design D. The weight of the truss C is increased by 43 kg. In procedure C, the optimization problem is changed radically with respect to the full problem. Optimization algorithm does not seek for smaller brace profiles by contraction since the brace profiles are fixed. Thus, geometric changes are not favorable with respect to the full problem, that is utilized in post sizing.

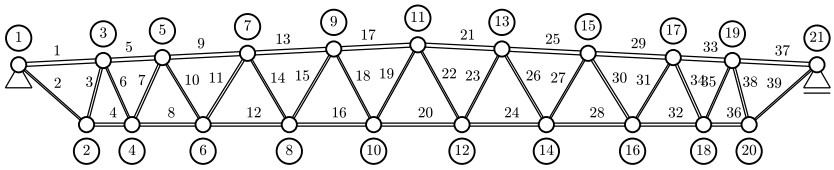

Figure 5.10 *Approach C, $W^* = 973$ kg.*

Table 5.13 *Approach C design, utilization ratios.*

Member	Profile	W [kg]	$U_{t,S}$ [%]	$U_{t,B}$ [%]
1, 37	120 × 6.0	52.8	22.76	66.82
2, 39	50 × 5.0	17.8	94.12	-
3, 38	70 × 4.0	15.9	53.07	93.91
4, 36	90 × 4.0	14.3	40.79	-
5, 33	120 × 6.0	36.9	22.03	30.68
6, 35	50 × 3.0	9.0	79.79	-
7, 34	70 × 4.0	17.6	42.68	84.69
8, 32	90 × 4.0	22.4	60.75	-
9, 29	120 × 6.0	53.2	32.94	66.74
10, 31	50 × 3.0	10.0	57.45	-
11, 30	70 × 3.0	15.5	40.23	91.99
12, 28	90 × 4.0	27.2	79.14	-
13, 25	120 × 6.0	53.8	39.40	81.31
14, 27	50 × 3.0	10.5	26.06	-
15, 26	60 × 3.0	13.7	21.53	66.03
16, 24	90 × 4.0	26.6	87.19	-
17, 21	120 × 6.0	52.5	40.80	81.18
18, 23	50 × 3.0	10.9	2.70	10.86
19, 22	50 × 3.0	11.6	2.52	-
20	90 × 4.0	27.8	86.44	-

In examples A, B and D the upper chord weight remains the same. In design C it increases 77 kg. This is again due to difficulties discussed earlier.

Designs A and B are identical. This shows that optimization process is not altered by reduction of big and small profiles, on this particular application. Most common roof truss geometries are simple. Furthermore, if the design domain is very narrow, then by engineering reasoning it is possible to determine which profiles are not potential alternatives and can be dropped from the optimization.

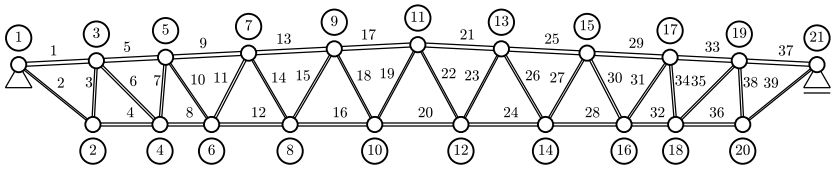

Figure 5.11 *Approach D, $W^* = 899$ kg.*

Table 5.14 *Approach D design, utilization ratios.*

Member	Profile	W [kg]	$U_{t,S}$ [%]	$U_{t,B}$ [%]
1, 37	120 × 5.0	41.0	33.44	100.00
2, 39	50 × 5.0	18.8	99.83	-
3, 38	70 × 4.0	15.3	51.75	88.31
4, 36	90 × 4.0	21.1	38.09	-
5, 33	120 × 5.0	36.6	32.18	51.41
6, 35	70 × 3.0	16.6	70.43	-
7, 34	70 × 3.0	12.4	50.15	88.74
8, 32	90 × 4.0	16.3	61.74	-
9, 29	120 × 5.0	43.9	40.77	81.14
10, 31	50 × 3.0	10.4	58.53	-
11, 30	70 × 3.0	14.8	37.81	81.66
12, 28	90 × 4.0	24.7	79.42	-
13, 25	120 × 5.0	45.3	47.93	100.00
14, 27	50 × 3.0	10.5	25.78	-
15, 26	60 × 3.0	13.7	21.30	65.19
16, 24	90 × 4.0	26.7	87.34	-
17, 21	120 × 5.0	44.1	49.50	99.44
18, 23	50 × 3.0	10.9	2.80	11.32
19, 22	50 × 3.0	11.6	2.60	-
20	90 × 4.0	27.2	86.57	-

5.4 Discussion

The exclusion of joint strength constraints is notable flaw in the approach proposed in this thesis. Considering joint strength constraints in the optimization might lead up to 15 % increase in truss weight according to Roxane et al. (2015). Joint constraints pose a problem for the sizing approach taken in this study, since all the constraints should be linear. For the same reason, chord bending moment from joint eccentricity is not considered in the implementation.

It should be mentioned that calculation time is strongly dependent on the implementation, available computational capacity and utilized computing environment. However, calculation time can serve as an indicator of applicability of the optimization procedure for modern designer.

6. CONCLUSIONS

The primary purpose of this thesis was to devise a new formulation for truss discrete geometry optimization problem to facilitate the development of practical design tool. Secondary purpose was to investigate the possibilities of geometry optimization on typical roof trusses. Thirdly, the usage of high-strength steel was also included in the study. Implicit programming was chosen as a basis of the approach combined with the MILP formulation for lower level problem solving. Proposed implementation gives a simple sizing problem that can be effectively solved using modern branch-and-cut solvers. The main advantage of this formulation is that it appears to be robust and the size of the lower level problem remains moderate as the number of variables is divided between upper and lower level problems resulting in reduced evaluation time.

Most of the prevailing design conditions were included in the problem solving increasing the quality of the solution by providing design that comply with the prevailing building codes. Thus, solution is applicable for practicing engineer.

Fast calculation time is an asset considering time and cost pressure in structural design. Therefore strict time limit was set for the computing. Then various computation procedures were developed to investigate the possibilities of reducing the problem size while maintaining the quality of the results. This led to trade-off between calculation time and weight reduction. As a result of procedure comparison one was selected to be the most suitable for the studied application. Calculation times were discovered to be serviceable.

Even though implementation was found to be reliable, it became evident, that with bigger problem sizes the calculation times begun to increase. Furhermore, including several loading conditions and vast profile libraries including several steel grades might increase computation time remarkably.

6.1 Further research

There are several options for future research directions.

Most obvious and direct development would be implementing cost function into the optimization. In industrial activity capital is the driving force and savings from the costs benefits all parties. Also note that minimum weight and cost often correlates with the minimal environmental effect.

In this thesis the SAND formulation was chosen for the lower level problem formulation. This led to problems nonlinear constraints discussed in Section 5.4. Other available methods for sizing optimization should be investigated in the framework of implicit programming approach. For instance, NAND formulation where structural analysis is solved *a priori* sizing optimization would tackle above-mentioned issues in lower level problem formulation. Furhermore, replacing MILP formulation by simple listing task combined with the NAND formulation might provide efficient approach.

Second research direction might be related to combined topology and sizing optimization in the context of implicit programming approach. MILP formulation, which has proven to be effective in topology optimization, combined with geometry optimization provides intriguing possibilities, especially when the geometry is not strictly limited.

BIBLIOGRAPHY

Achtziger, W. (2007). "On simultaneous optimization of truss geometry and topology". In: *Struct. Multidiscip. Optim* 33, pp. 285 –304.

Dorn, W., R. Gomory, and M. Greenberg (1964). "Automatic Design of Optimal Structures". In: *J. Mec* 3, pp. 25–52.

EN 1993–1–1 (2005). *Eurocode 3: Design of Steel Structures. Part 1-1: General rules and rules for buildings*. CEN.

EN 1993–1–12 (2005). *Eurocode 3: Design of steel structures. Part 1-12: Additional rules for the extension of EN 1993 up to steel grades S700*. CEN.

EN 1993–1–8 (2005). *Eurocode 3: Design of steel structures. Part 1-8: Design of joints*. CEN.

Ghattas, O. and I. E. Grossmann (1991). "MINLP and MILP strategies for discrete sizing structural optimization problems". In: *Proceedings of the 10th conference on electronic computation*. Ed. by O. Ural and T. L. Wang. ASCE, pp. 197–204.

Grossmann, I. E., V. T. Voudouris, and O. Ghattas (1992). "Mixed-integer linear programming reformulations for some nonlinear discrete design optimization problems". In: *Recent advances in global optimization*. Ed. by C. A. Floudas and P. M. Pardalos. Princeton University Press, pp. 478–512.

Gurobi Optimization, Inc. (2017). *Gurobi Optimizer Reference Manual*. `http://www.gurobi.com`.

Hafka, R. T. and Z. Gürdal (1992). *Elements of Structural Optimization, Third Revised and Expanded Edition*. Kluwer Academic Publisher.

Kirsch, U. (1981). *Optimum Structural Design. Consepts, Methods and Applications*. McGraw-Hill Book Company.

MathWorks, Inc. (2017). *Matlab Reference Manual*.

Mela, K. (2013). "Mixed Variable Formulations for Truss Topology Optimization". PhD thesis. Tampere University of Technology.

– (2014). In: *Struct Multidisc Optim* 50, pp. 1037–1049.

Pedersen, P. (1972). "Optimal Layout of Multi-Purpose Trusses". In: *Computers & Structures* 2, pp. 695–712.

Rasmussen, M. and M. Stolpe (2008). "Global optimization of discrete truss topology design problems using a parallel cut-and-branch method". In: *Compu. Struct* 86, pp. 1527–1538.

Roxane, v., G. Lombaert, and M. Schevenels (2015). "Global Size Optimization of Statically Determinate Trusses Considering Displacement, Member, and Joint Constraints". In: *Journal of Structural Engineering* 142, pp. 1–13.

SSAB (2017). *SSAB Domex Tube Double Grade*.

Wolsey, L. A. (1998). *Integer Programming*. John Wiley & Sons.

APPENDIX A. PROFILE DATA

In the following, profile data utilized in numerical calculations is presented. Profiles corresponding to steel grades S420, S550 and S700 are shown in respective tables. It is checked, that all internal parts of profiles belong to the cross-section class 1 or 2 according to section 5.5 of EN 1993–1–1 2005.

Table 1 *Profile data for steel grade S420.*

Profile	H [mm]	T [mm]	A [10^2 mm^2]	I [10^4 mm^4]
1	25	3.0	2.41	1.84
2	30	3.0	3.01	3.50
3	40	3.0	4.21	9.32
4	40	4.0	5.35	11.07
5	50	3.0	5.41	19.47
6	50	4.0	6.95	23.74
7	50	5.0	8.36	27.04
8	60	3.0	6.61	35.13
9	60	4.0	8.55	43.55
10	60	5.0	10.36	50.49
11	70	3.0	7.81	57.53
12	70	4.0	10.15	72.12
13	70	5.0	12.36	84.63
14	80	3.0	9.01	87.84
15	80	4.0	11.75	111.04
16	80	5.0	14.36	131.44
17	80	6.0	16.83	149.18
18	90	3.0	10.21	127.28
19	90	4.0	13.35	161.92
20	90	5.0	16.36	192.93
21	90	6.0	19.23	220.48
22	100	4.0	14.95	226.35
23	100	5.0	18.36	271.10
24	100	6.0	21.63	311.47
25	100	7.1	24.65	340.13
26	100	8.0	27.24	365.94
27	110	4.0	16.55	305.94
28	110	5.0	20.36	367.95
29	110	6.0	24.03	424.57
30	120	4.0	18.15	402.28

continued from previous page

Profile	H [mm]	T [mm]	A $[10^2$ mm$^2]$	I $[10^4$ mm$^4]$
31	120	5.0	22.36	485.47
32	120	6.0	26.43	562.16
33	120	7.1	30.33	623.52
34	120	8.0	33.64	676.88
35	120	10.0	40.57	776.81
36	140	5.0	26.36	790.56
37	140	6.0	31.23	920.43
38	140	7.1	36.01	1031.71
39	140	8.0	40.04	1126.77
40	140	8.8	43.52	1205.03
41	140	10.0	48.57	1311.67
42	150	5.0	28.36	982.12
43	150	6.0	33.63	1145.91
44	150	7.1	38.85	1289.70
45	150	8.0	43.24	1411.83
46	150	8.8	47.04	1513.12
47	150	10.0	52.57	1652.53
48	150	12.5	62.04	1817.44
49	160	5.0	30.36	1202.36
50	160	6.0	36.03	1405.48
51	160	7.1	41.69	1587.41
52	160	8.0	46.44	1741.23
53	160	8.8	50.56	1869.59
54	160	10.0	56.57	2047.67
55	160	12.5	67.04	2275.04
56	180	6.0	40.83	2036.52
57	180	7.1	47.37	2313.34
58	180	8.0	52.84	2545.86
59	180	8.8	57.60	2741.73
60	180	10.0	64.57	3016.80
61	180	12.5	77.04	3406.43
62	200	7.1	53.05	3232.22
63	200	8.0	59.24	3566.25
64	200	8.8	64.64	3849.59
65	200	10.0	72.57	4251.06
66	200	12.5	87.04	4859.42
67	220	7.1	58.73	4366.78
68	220	8.0	65.64	4828.01
69	220	8.8	71.68	5221.35
70	220	10.0	80.57	5782.46
71	220	12.5	97.04	6673.98
72	250	8.0	75.24	7229.20
73	250	8.8	82.24	7835.39

continued from previous page

Profile	H [mm]	T [mm]	A $[10^2$ mm$^2]$	I $[10^4$ mm$^4]$
74	250	10.0	92.57	8706.67
75	250	12.5	112.04	10161.31
76	260	8.0	78.44	8178.02
77	260	8.8	85.76	8869.18
78	260	10.0	96.57	9864.65
79	260	12.5	117.04	11547.88
80	300	10.0	112.57	15519.37
81	300	12.5	137.04	18348.13

Table 2 *Profile data for steel grade S550.*

Profile	H [mm]	T [mm]	A $[10^2$ mm$^2]$	I $[10^4$ mm$^4]$
1	30	3.0	3.01	3.50
2	40	3.0	4.21	9.32
3	40	4.0	5.35	11.07
4	50	3.0	5.41	19.47
5	50	4.0	6.95	23.74
6	60	3.0	6.61	35.13
7	60	4.0	8.55	43.55
8	60	5.0	10.36	50.49
9	70	3.0	7.81	57.53
10	70	4.0	10.15	72.12
11	70	5.0	12.36	84.63
12	80	3.0	9.01	87.84
13	80	4.0	11.75	111.04
14	80	5.0	14.36	131.44
15	80	6.0	16.83	149.18
16	90	4.0	13.35	161.92
17	90	5.0	16.36	192.93
18	90	6.0	19.23	220.48
19	100	4.0	14.95	226.35
20	100	5.0	18.36	271.10
21	100	8.0	27.24	365.94
22	110	4.0	16.55	305.94
23	120	5.0	22.36	485.47
24	120	6.0	26.43	562.16
25	120	8.0	33.64	676.88
26	140	5.0	26.36	790.56
27	140	6.0	31.23	920.43
28	140	8.0	40.04	1126.77
29	140	10.0	48.57	1311.67
30	150	6.0	33.63	1145.91

continued from previous page

Profile	H [mm]	T [mm]	A $[10^2$ mm$^2]$	I $[10^4$ mm$^4]$
31	150	8.0	43.24	1411.83
32	150	10.0	52.57	1652.53
33	160	6.0	36.03	1405.48
34	160	8.0	46.44	1741.23
35	160	10.0	56.57	2047.67
36	160	12.5	67.04	2275.04
37	180	8.0	52.84	2545.86
38	180	10.0	64.57	3016.80
39	180	12.5	77.04	3406.43
40	200	8.0	59.24	3566.25
41	200	10.0	72.57	4251.06
42	200	12.5	87.04	4859.42
43	250	10.0	92.57	8706.67

Table 3 *Profile data for steel grade S700.*

Profile	H [mm]	T [mm]	A $[10^2$ mm$^2]$	I $[10^4$ mm$^4]$
1	40	3.0	4.21	9.32
2	50	3.0	5.41	19.47
3	60	3.0	6.61	35.13
4	60	4.0	8.55	43.55
5	70	3.0	7.81	57.53
6	70	4.0	10.15	72.12
7	70	5.0	12.36	84.63
8	80	4.0	11.75	111.04
9	80	5.0	14.36	131.44
10	80	6.0	16.83	149.18
11	90	4.0	13.35	161.92
12	90	5.0	16.36	192.93
13	100	4.0	14.95	226.35
14	100	5.0	18.36	271.10
15	100	6.0	21.63	311.47
16	100	8.0	27.24	365.94
17	120	5.0	22.36	485.47
18	120	6.0	26.43	562.16
19	120	8.0	33.64	676.88
20	140	6.0	31.23	920.43
21	140	8.0	40.04	1126.77
22	140	10.0	48.57	1311.67
23	160	8.0	46.44	1741.23
24	160	10.0	56.57	2047.67
25	180	8.0	52.84	2545.86

continued from previous page

Profile	H [mm]	T [mm]	A $[10^2$ mm$^2]$	I $[10^4$ mm$^4]$
26	180	10.0	64.57	3016.80
27	200	8.0	59.24	3566.25
28	200	10.0	72.57	4251.06
29	220	10.0	80.57	5782.46
30	250	10.0	92.57	8706.67

APPENDIX B. NODAL COORDINATES

Horizontal and vertical nodal coordinates are presented for initial design (Init.) and for optimum design (Opt.).

Table 4 *Nodal coordinates of truss A.*

Node no.	Horizontal [mm]		Vertical [mm]		
	Init.	Opt.	Init.	Opt.	
1	0	0	0	0	fixed
2	1200	1992	-1800	-1800	
3	2400	2488	120	124	
4	3600	3920	-1800	-1800	
5	4800	4688	240	234	
6	6000	6256	-1800	-1800	
7	7200	7032	360	352	
8	8400	8272	-1800	-1800	
9	9600	9488	480	474	
10	10800	10704	-1800	-1800	
11	12000	12000	600	600	fixed
12	13200	13296	-1800	-1800	
13	14400	14512	480	474	
14	15600	15728	-1800	-1800	
15	16800	16968	360	352	
16	18000	17744	-1800	-1800	
17	19200	19312	240	234	
18	20400	20080	-1800	-1800	
19	21600	21512	120	124	
20	22800	22008	-1800	-1800	
21	24000	24000	0	0	fixed

Table 5 *Nodal coordinates of truss B.*

Node no.	Horizontal [mm]		Vertical [mm]		
	Init.	Opt.	Init.	Opt.	
1	0	0	0	0	fixed
2	1200	1992	-1800	-1800	
3	2400	2488	120	124	
4	3600	3920	-1800	-1800	
5	4800	4688	240	234	
6	6000	6256	-1800	-1800	
7	7200	7032	360	352	
8	8400	8272	-1800	-1800	
9	9600	9488	480	474	
10	10800	10704	-1800	-1800	
11	12000	12000	600	600	fixed
12	13200	13296	-1800	-1800	
13	14400	14512	480	474	
14	15600	15728	-1800	-1800	
15	16800	16968	360	352	
16	18000	17744	-1800	-1800	
17	19200	19312	240	234	
18	20400	20080	-1800	-1800	
19	21600	21512	120	124	
20	22800	22008	-1800	-1800	
21	24000	24000	0	0	fixed

Table 6 *Coordinates of a truss C.*

Node no.	Horizontal [mm]		Vertical [mm]		
	Init.	Opt.	Init.	Opt.	
1	0	0	0	0	fixed
2	1200	2040	-1800	-1800	
3	2400	2544	120	127	
4	3600	3408	-1800	-1800	
5	4800	4321	240	216	
6	6000	5544	-1800	-1800	
7	7200	6880	360	344	
8	8400	8136	-1800	-1800	
9	9600	9472	480	474	
10	10800	10672	-1800	-1800	
11	12000	12000	600	600	fixed
12	13200	13328	-1800	-1800	
13	14400	14528	480	474	
14	15600	15864	-1800	-1800	
15	16800	17120	360	344	
16	18000	18456	-1800	-1800	
17	19200	19679	240	216	
18	20400	20592	-1800	-1800	
19	21600	21456	120	127	
20	22800	21960	-1800	-1800	
21	24000	24000	0	0	fixed

Table 7 *Nodal coordinates of truss D.*

Node no.	Horizontal [mm]		Vertical [mm]		
	Init.	Opt.	Init.	Opt.	
1	0	0	0	0	fixed
2	1200	2232	-1800	-1800	
3	2400	2336	120	117	
4	3600	4248	-1800	-1800	
5	4800	4416	240	221	
6	6000	5800	-1800	-1800	
7	7200	6912	360	346	
8	8400	8160	-1800	-1800	
9	9600	9488	480	474	
10	10800	10704	-1800	-1800	
11	12000	12000	600	600	fixed
12	13200	13296	-1800	-1800	
13	14400	14512	480	474	
14	15600	15840	-1800	-1800	
15	16800	17088	360	346	
16	18000	18200	-1800	-1800	
17	19200	19584	240	221	
18	20400	19752	-1800	-1800	
19	21600	21664	120	117	
20	22800	21768	-1800	-1800	
21	24000	24000	0	0	fixed